CHAPTER 4

APPLICATION OF THE LAYERED STABILIZED FLOW MODEL

Five cases were investigated in order to verify the capability of the Layered Stabilized Flow Model in predicting original gas in place (OGIP). Three were hypothetical cases with production data generated from either a reservoir simulator or a well test simulation program. The other two are actual field cases with the production data taken from two wells in the Gulf of Thailand. The model generation, results and analysis of the results will be discussed for each case.

4.1 Case 1: Simulated Two-Layer Reservoir

The first simulated case is for a two-layered commingled gas reservoir with very low permeability. This case was taken from the 1996 El-Banbi and Wattenbarger paper[1] where a gas reservoir simulator was used to generate a hypothetical production rate history. The intent of performing the analysis on this case is to validate if the model is correctly setup. If the results obtained from running the LSFM program match the results from the paper, the confidence in using the model can be established.

4.1.1 Reservoir and Fluid Properties

The reservoir and fluid properties are presented in Table 4.1.

Table 4.1: Reservoir and fluid property data (Case 1).

Properties	Layer 1	Layer 2
Area, acres	80	80
Thickness, ft	50	50
Porosity, fraction	0.1	0.1
Initial pressure, psia	2500	2500
BHFP, psia	500	500
Temperature, deg F	150	150
Gas gravity	0.6	0.6
Formation compressibility, psi^{-1}	3.0E-06	3.0E-06
Permeability, mD	10	1

Examination of Table 4.1 shows that all of the reservoir and fluid properties for both layers are the same except for the layer permeability. The permeability contrast between the two layers is one order of magnitude, with Layer 1 being the more permeable layer.

Both layers have the same initial reservoir pressure of 2500 psia and have been flowing against a constant bottomhole pressure of 500 psia.

4.1.2 Production Data

The production profile of this two-layered reservoir is presented in Fig. 4.1. The graph shows production from month 1 until month 100 (day 30 to day 3000). The calibration period or the period at which the history matching will be performed is also marked in the graph. The calibration period covers the production data from month 14 to month 40 (day 420 to day 1200).

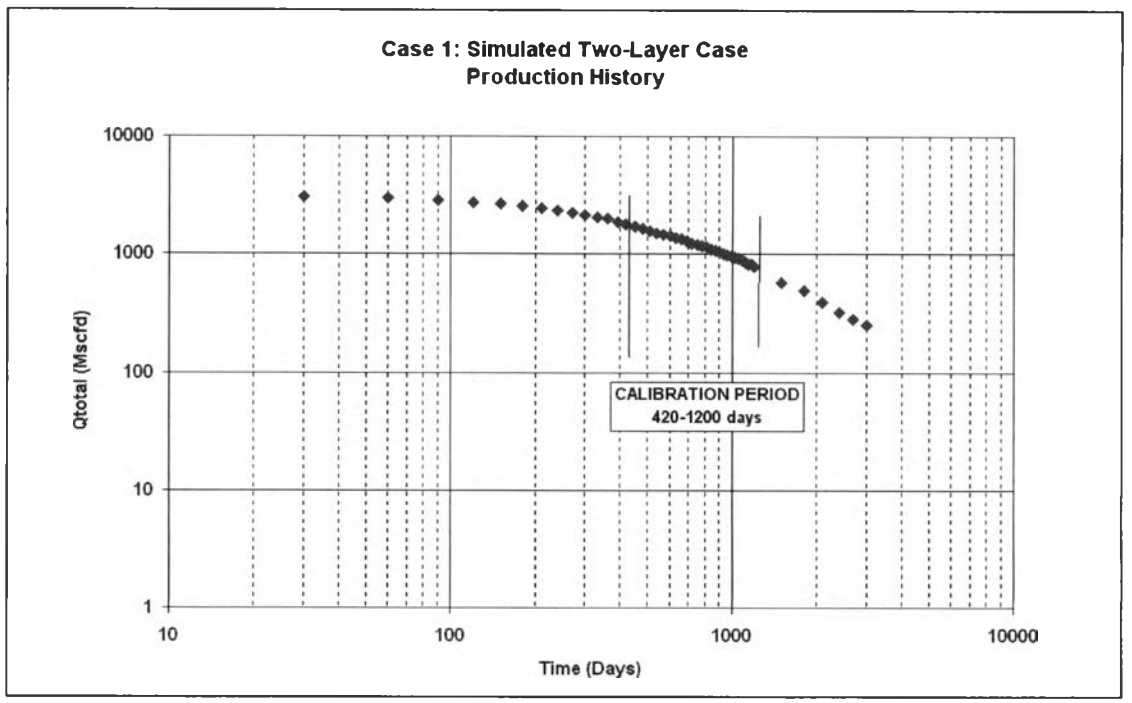

Figure 4.1: Production history for Case 1.

4.1.3 Normalized Pseudo-pressure Table

As mentioned earlier, both layers are producing at a constant bottomhole pressure of 500 psi. Except for permeability, all reservoir and fluid properties are the same for the two layers. Therefore, the normalized pseudo-pressure for both layers should be the same and only one normalized pseudo-pressure table would be constructed and used for both layers.

To set up the normalized pseudo-pressures, gas deviation factors and gas viscosities are calculated at pressure values starting from the reference pressure (initial pressure) of 2500 psia to atmospheric pressure. The z-factors are calculated using Eq. 3.23 while the gas viscosities are calculated using Eq. 3.29.

The normalized pseudo-pressure table used for Layers 1 and 2 is presented in Table A.1 (see Appendix). The corresponding pseudo-pressure graph is given in Fig.

A.1 (see Appendix). For both layers, the calculated flowing bottom-hole pressure in terms of the normalized pseudo-pressure is 1168 psia.

4.1.4 History Matching

Once the gas properties and the normalized pseudo-pressure tables were prepared, the history matching was then performed. The critical part in the history matching using the LSFM program is to come up with reasonable initial guesses for the unknown parameters G_k, J_k and G_{pk}'. Otherwise, the Gauss-Marquardt technique takes a long time to converge or it may converge at a wrong minimum.

For this two-layer case, six parameters need to be estimated. As a result, several combinations of initial guesses of the unknown parameters can be made to fit the model rate equation to the actual rate data. As such, there is a probability of non-uniqueness in the solution. The following considerations were used as a guide to make the initial estimation as accurate as possible:

1. Knowing that Layer 1 is more permeable than Layer 2, the initial production is intuitively coming mainly from Layer 1. Therefore, a higher percentage of the initial total cumulative production G_p' is allocated to Layer 1.
2. As a result of the higher permeability of Layer 1, the productivity index of Layer 1, J_{g1}, is also expected to be higher than that of Layer 2. The productivity index values affect the slope of the model rate equation and give an indication of how fast pressure depletion is occurring in the layers. Therefore, it follows that the total production will initially be controlled by the more permeable Layer 1.

After making the initial guesses and adjusting and refining them as needed, the history matching with the LSFM program was done.

4.1.5 Results and Discussion

The comparison of the results of the history matching using the LSFM program and the El-Banbi and Wattenbarger paper is presented in Table 4.2. The graph of the history match is given in Fig. 4.2.

Table 4.2: Comparison of the G and J_g calculated from the LSFM program and the El-Banbi and Wattenbarger paper.

	OGIP (MMscf)	OGIP (MMscf)	Jg (scf/psi-d)	Jg (scf-cp/psi^2-d)
	LSFM Program	El-Banbi paper	LSFM Program	El-Banbi paper
Layer 1	2898.2	2903.4	2104.6	7.392E-03
Layer 2	2962.9	2931.3	698.1	7.652E-04

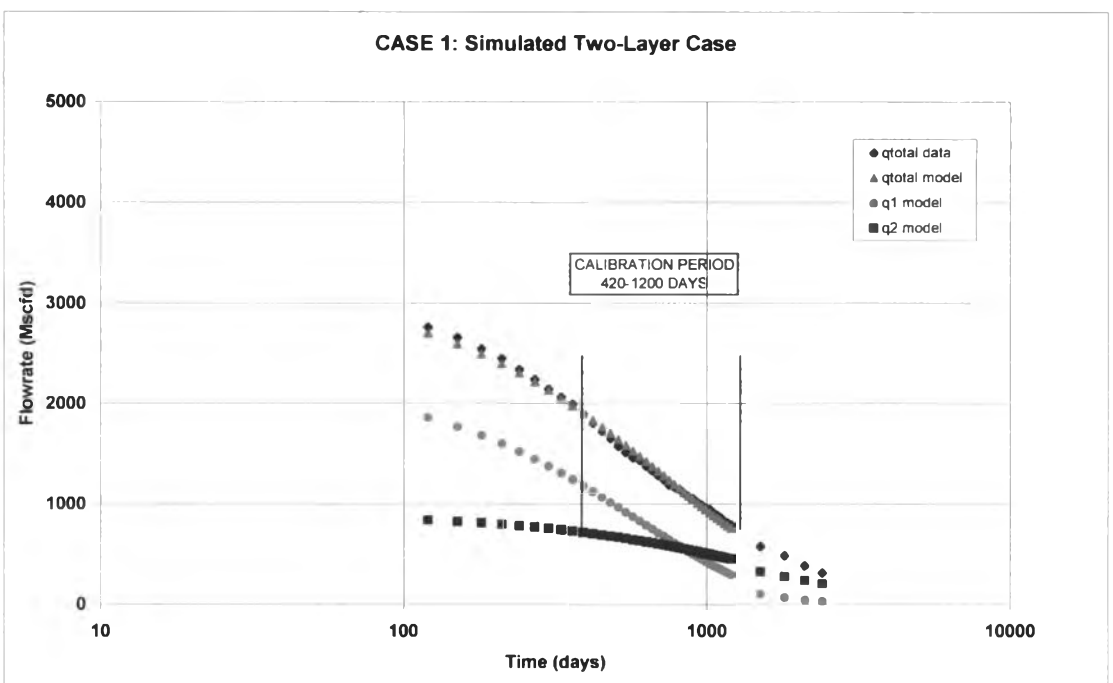

Figure 4.2: History matching result for Case 1.

From Fig. 4.2, it can be seen that Layer 1 is the major contributor to the production of this two-layered reservoir from the start of production until about the 30th month. Depletion in Layer 1 started to slow down from this period and Layer 2 started to contribute more. This is a typical characteristic of a commingled reservoir with a big permeability contrast.

Close examination of the model rate and the actual rate from Fig. 4.2 shows that the model rate equation seems to under predict the earlier and the later time data. This was probably the reason why El-Banbi and Wattenbarger chose to limit the calibration period from month 13 to month 36.

From Table 4.2, the OGIP values calculated from the LSFM program and the paper are very close with 0.2% and 1.02% difference for Layer 1 and Layer 2, respectively. The productivity indices have different values and units since the LSFM program used normalized pseudo-pressures while the paper used pseudo-pressures.

One reason that could explain the difference between the OGIP values is the difference in the calibration period used for the history matching. For this case, the calibration period used for the history matching was from month 14 to month 40 while the El-Banbi paper used month 13 to month 36. The difference may also have been due to the correlations used for calculating the gas deviation factors and viscosities which were then used for calculating the pseudo-pressures.

4.1.6 Sensitivity Runs

Several sensitivity runs were made to investigate the effect of the calibration period for the history matching. The production data were divided into 10-month and 20-month intervals. The calibration period for each sensitivity runs is given in Table 4.3.

Table 4.3: Calibration period for sensitivity runs

Sensitivity Run Number	Calibration Period
Run 1	4 to 24 months (20-month interval)
Run 2	14 to 34 months (20-month interval)
Run 3	24 to 44 months (20-month interval)
Run 4	4 to 14 months (10-month interval)
Run 5	14 to 24 months (10-month interval)
Run 6	24 to 34 months (10-month interval)
Run 7	34 to 44 months (10-month interval)

The results of the history matching for the sensitivity runs are given in Table 4.4 and Figs. 4.3 through 4.13.

Table 4.4: Results of sensitivity runs for Case 1.

Run Number	OGIP (MMscf) Layer 1	OGIP (MMscf) Layer 2	Jg (scf/psi-d) Layer 1	Jg (scf/psi-d) Layer 2
Run 1 4 to 24 months	2823.06	2837.82	2108.93	697.98
Run 2 14 to 34 months	2890.92	2952.27	2103.83	698.49
Run 3 24 to 44 months	2908.08	2968.03	2101.89	698.87
Run 4 4 to 14 months	2819.00	2833.97	2116.15	697.19
Run 5 14 to 24 months	2859.18	2886.89	2108.32	698.40
Run 6 24 to 34 months	2897.18	2964.06	2102.98	698.57
Run 7 34 to 44 months	2912.00	2968.00	2092.00	699.98

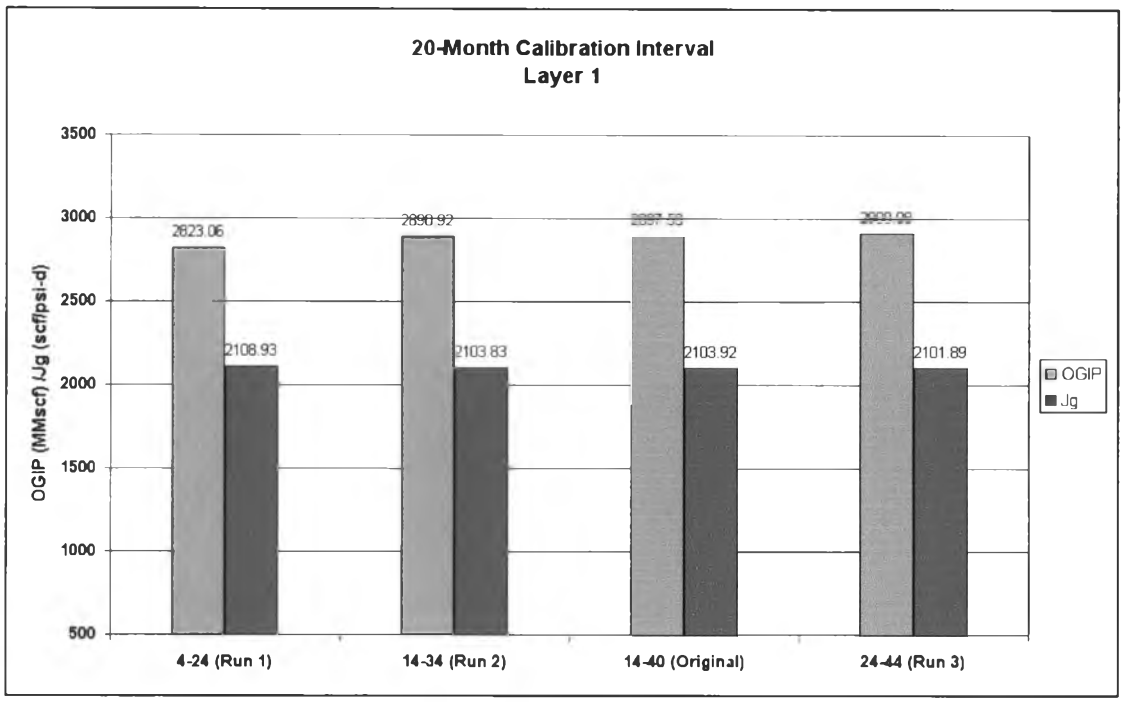

Figure 4.3: OGIP and J_g of Layer 1 at 20-month calibration intervals.

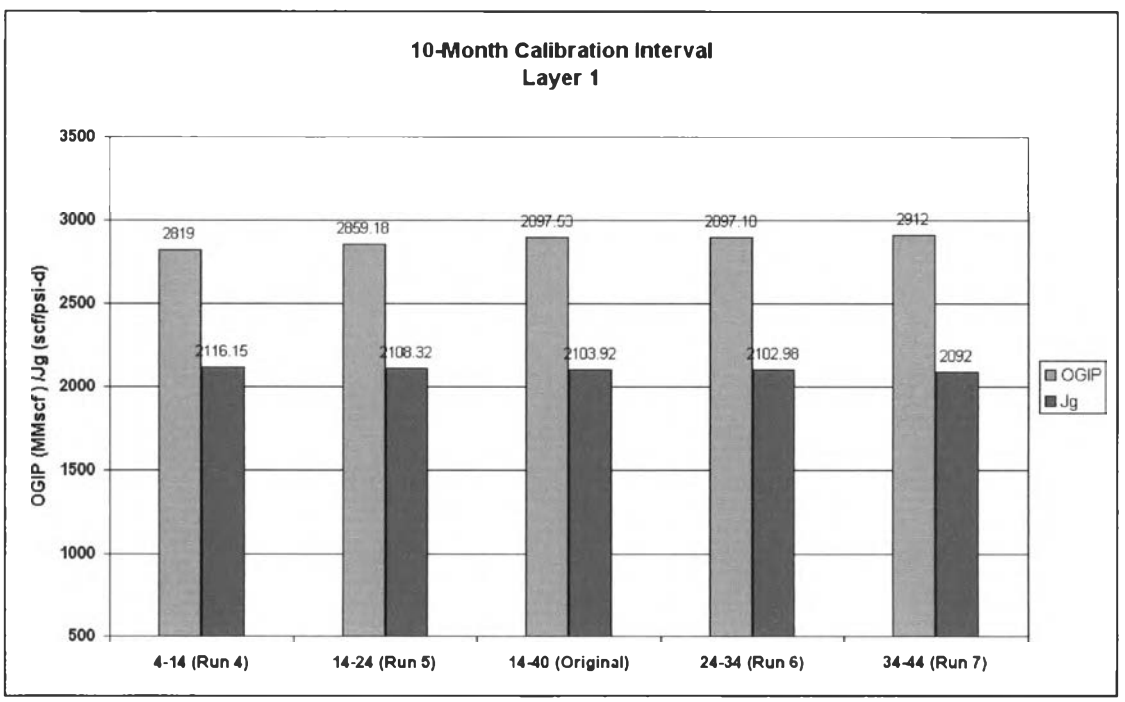

Figure 4.4: OGIP and J_g of Layer 1 at 10-month calibration intervals.

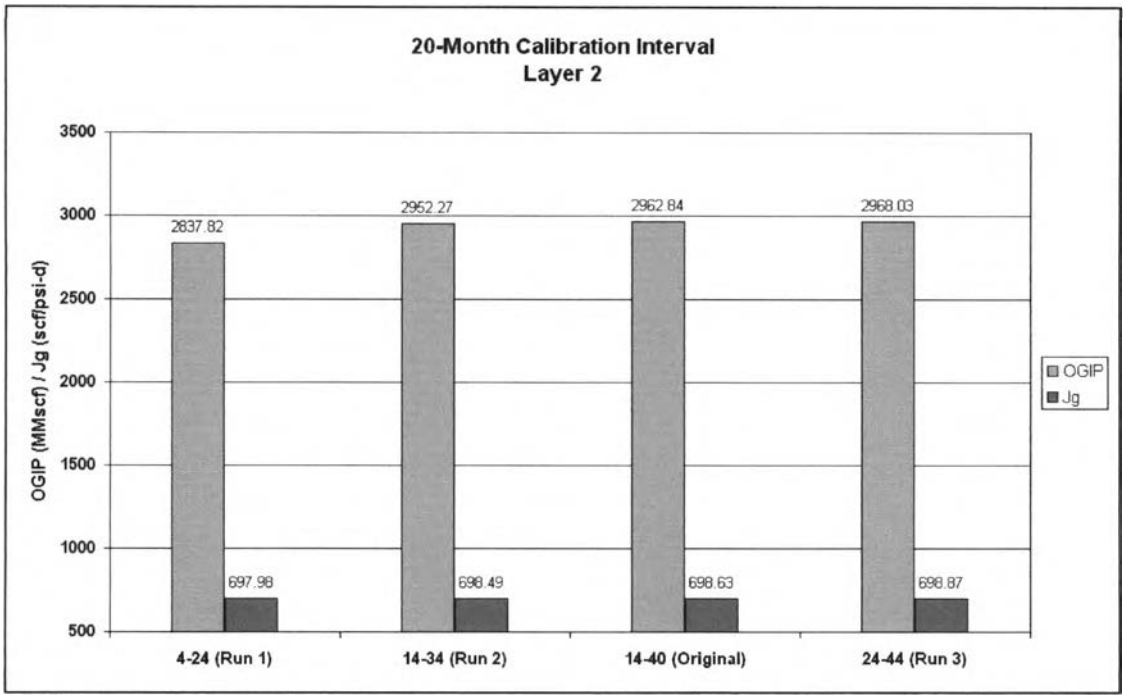

Figure 4.5: OGIP and J_g of Layer 2 at 20-month calibration intervals.

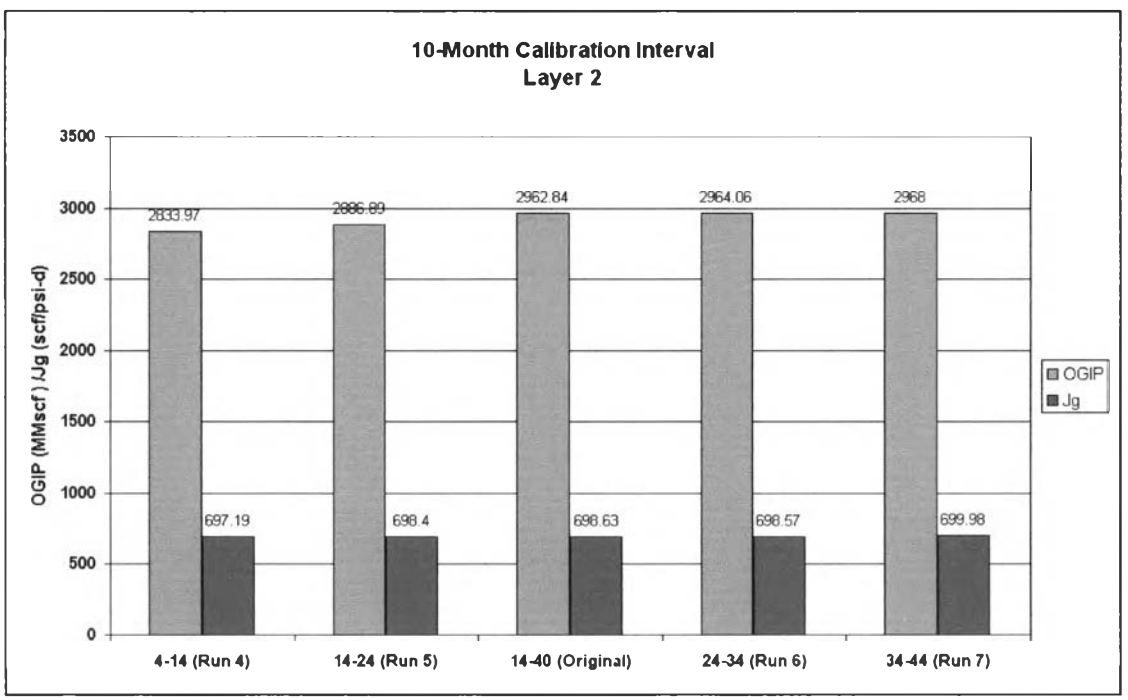

Figure 4.6: OGIP and J_g of Layer 2 at 10-month calibration intervals.

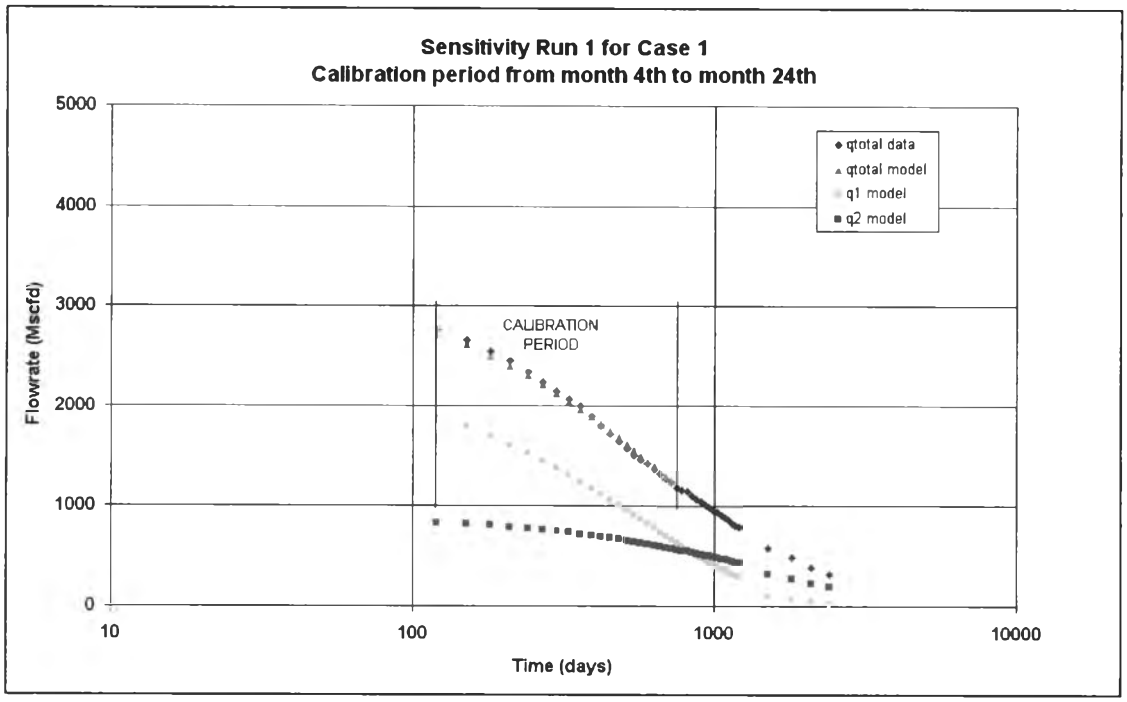

Figure 4.7: History matching result for Run 1.

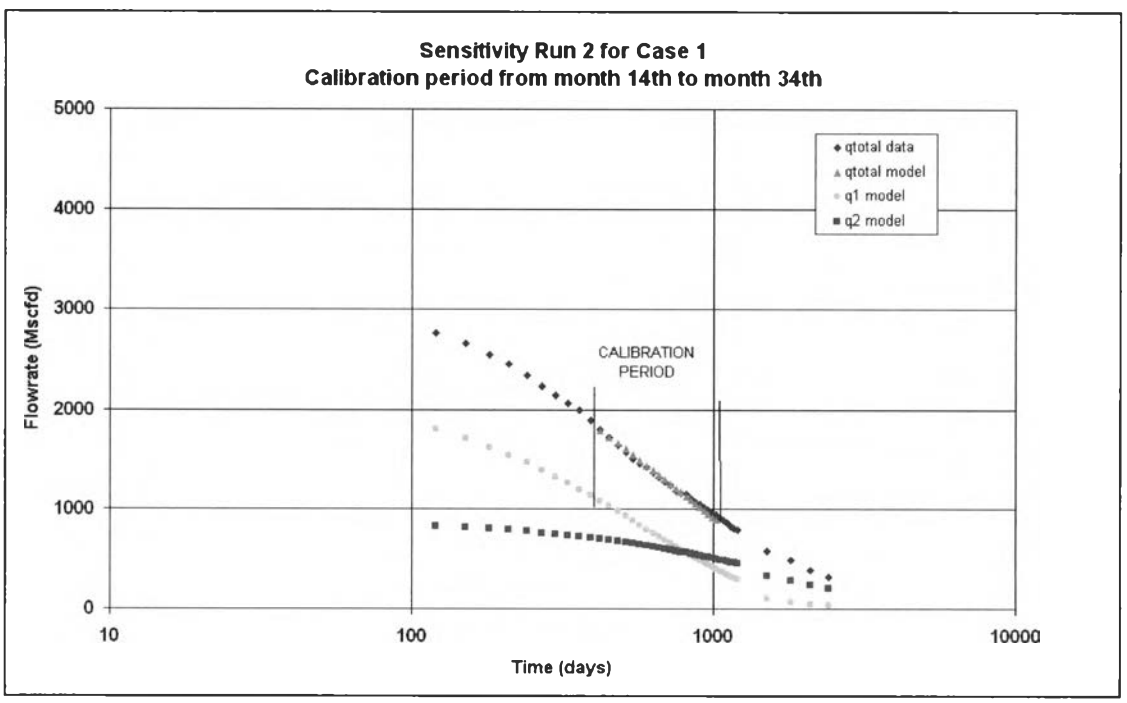

Figure 4.8: History matching result for Run 2.

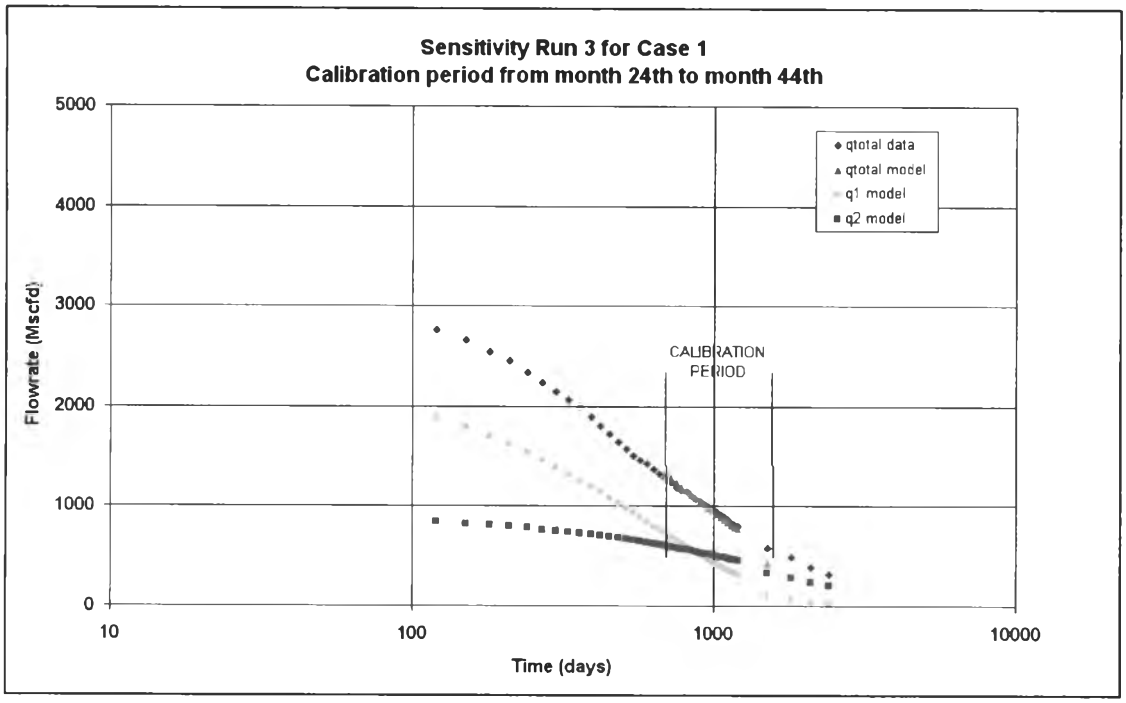

Figure 4.9: History matching result for Run 3.

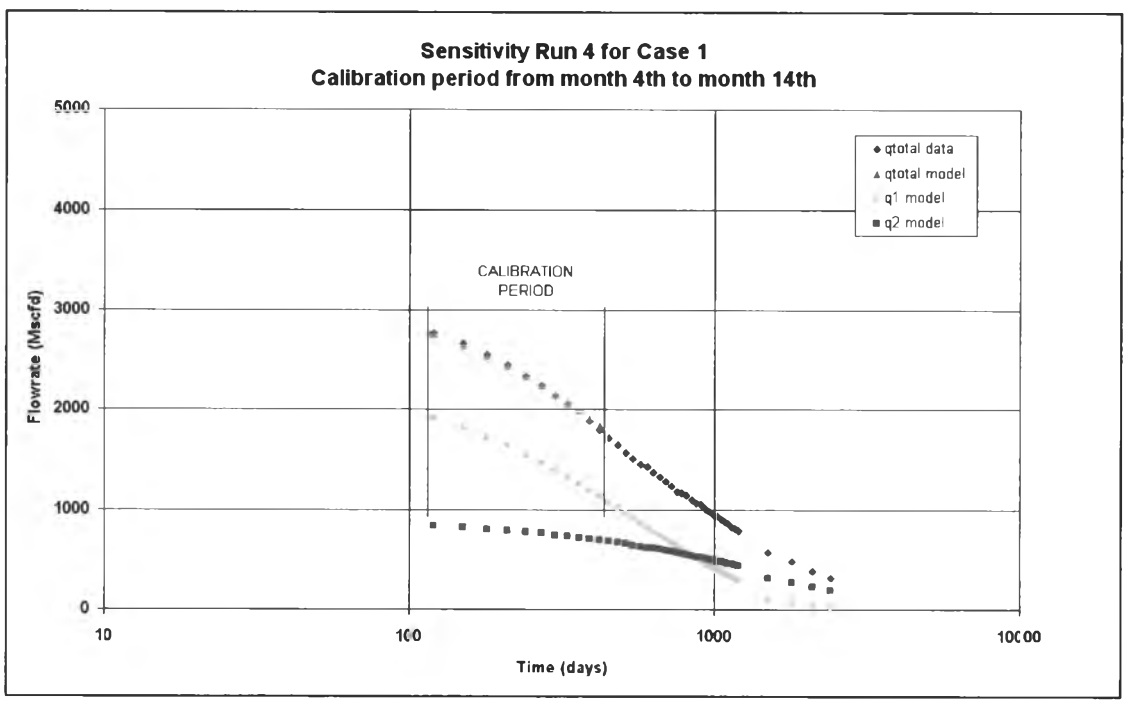

Figure 4.10: History matching result for Run 4.

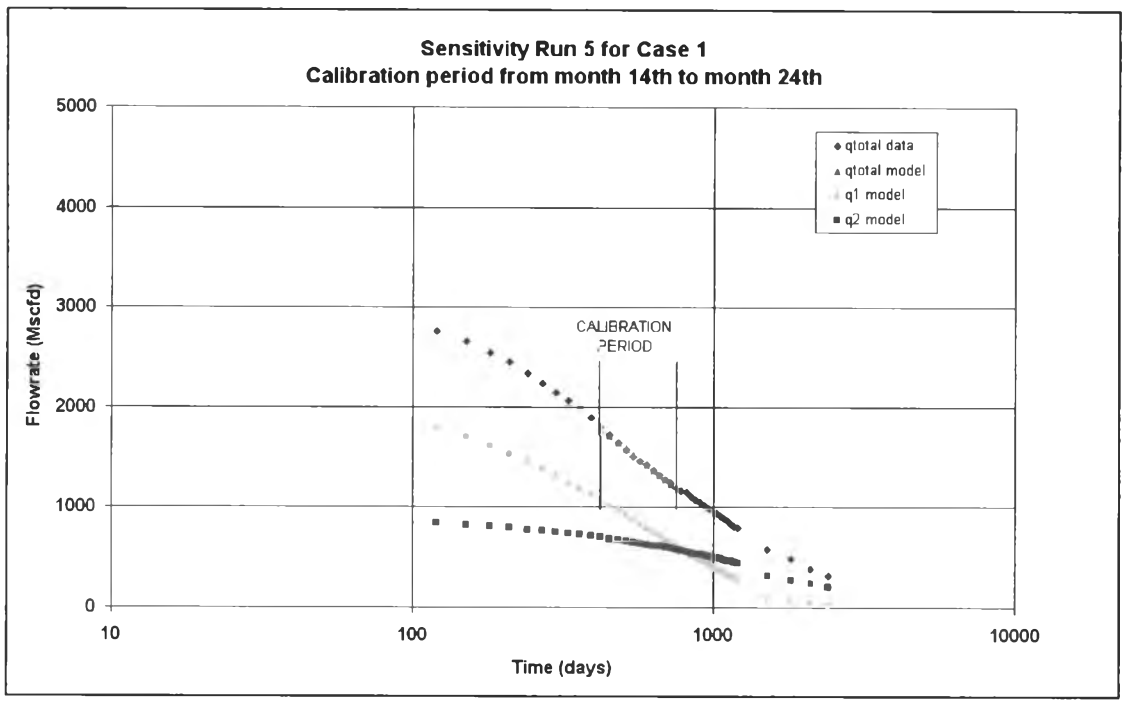

Figure 4.11: History matching result for Run 5.

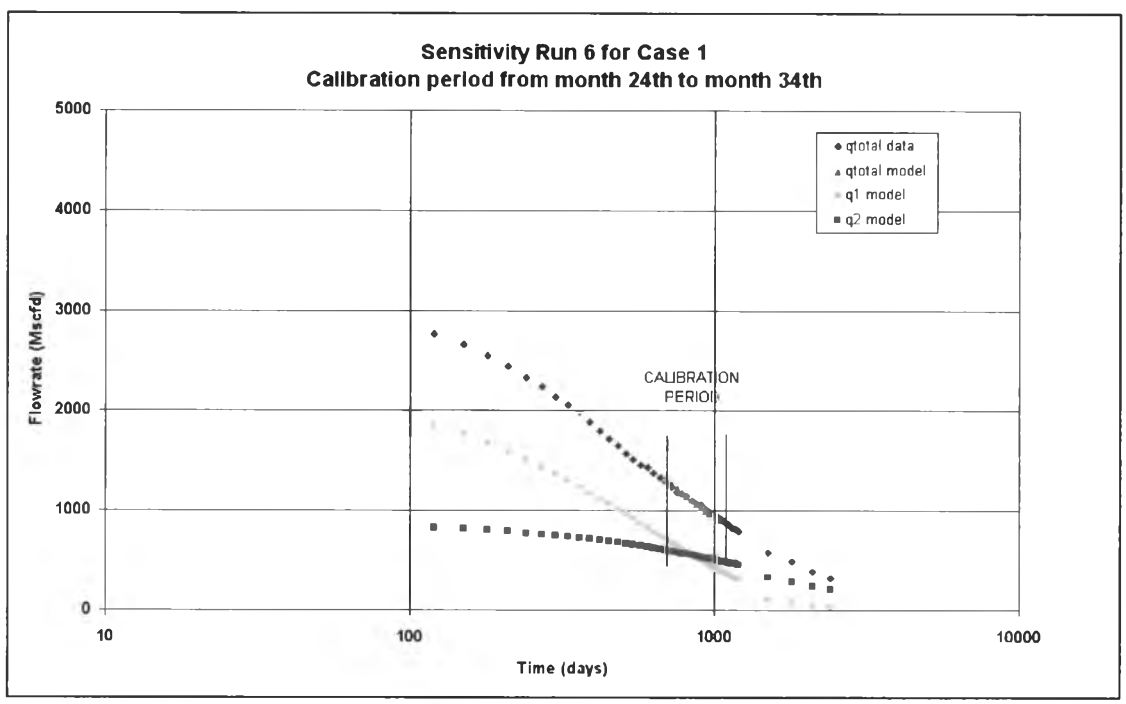

Figure 4.12: History matching result for Run 6.

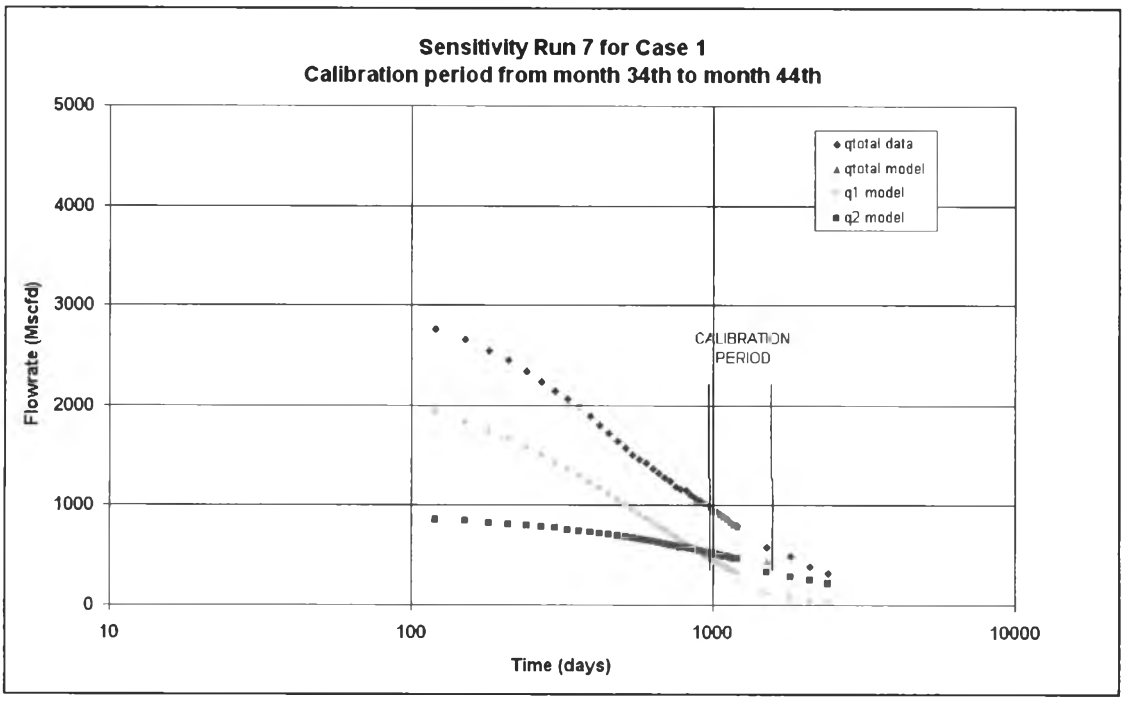

Figure 4.13: History matching result for Run 7.

From Figs. 4.3 and 4.4, it can be seen that the OGIP of Layer 1 shows lower values when the calibration period covers the early production period as evident from the results of Run 1, 4 and 5. The results from Run 2, 3, and 6 do not vary significantly from the result of the original run. Run 7 shows a slightly higher OGIP value which may have been attributed to the late time data used in the history-match. The J_g values of Layer 1 do not vary much in all the sensitivity runs although it can be seen that the runs that include early transient period show slightly higher values (see results from Run 1, 4 and 5).

Layer 2 shows a similar trend i.e., the OGIP values are underestimated from the results of Run 1, 4 and 5 (see Figs. 4.5 and 4.6). The values of the OGIP from the rest of the sensitivity runs (Runs 2, 3 and 6) are almost unvarying. The values of J_g of Layer 2 did not change substantially in all the sensitivity runs.

From these results, it can be seen that using earlier data seems to under-predict the OGIP. This is due to the fact that the earlier data may have not been beyond the

transient period. It is known that tight reservoirs are expected to have long transient periods and that inclusion of transient flow generally under predicts the OGIP. Conversely, the slightly higher OGIP values from Sensitivity Run 7 for both layers suggest that the late time data may tend to over-predict the OGIP.

Having calculated the OGIP values to be very similar to the El-Banbi paper, it can be concluded that the program was set-up correctly and can now be used for other cases for predicting OGIP.

4.2 Case 2: Simulated Four-Layer Reservoir with the Same Initial Reservoir Pressures

Case 2 is a simulated case in which the production rate and the flowing bottom hole pressure profiles were generated using *PanSystem*, a well test interpretation software [16]. The purpose of performing the history match on this simulated case is for further verification of the LSFM program. *PanSystem* calculates the flowing bottomhole pressure corresponding to the user-defined production rate history. In order to generate the flowing bottomhole pressures, the well and layer parameters need to be supplied for the simulation run. The *PanSystem* program is also capable of predicting the production rate contribution of each layer, thus making it an ideal program for verifying the results of the LSFM Program.

This simulated case is for a four-layer gas reservoir with moderate permeability ranging from 5 to 30 mD. The effect of skin is also investigated in this run. To see the effect of skin, a skin factor was included in layer 2, the most permeable layer.

PanSystem requires layer boundary information which allows the drainage area of each layer to be defined and hence, the gas in place to be defined as well. All four layers were modeled as a closed, no flow boundary system.

For this case, all layers were modeled to have the same initial reservoir pressures at the onset of production. The effect of having different initial layer pressures will be investigated in Case 3.

4.2.1 Reservoir and Fluid Properties

Tables 4.5A through 4.5C provides all the reservoir and fluid parameters used as input data for the PanSystem program in order to generate the flowing bottomhole pressure that corresponds to the production rate defined.

Table 4.5A: Reservoir and fluid property data for Case 2.

	Layer 1	Layer 2	Layer 3	Layer 4
Formation thickness, ft	20	10	30	15
Average formation porosity, fraction	0.21	0.22	0.19	0.26
Water saturation, fraction	0.46	0.41	0.40	0.48
Gas saturation, fraction	0.54	0.59	0.60	0.52
Formation compressibility, psi^{-1}	3.5737e-6	3.5054e-6	3.7253e-6	3.2706e-6
Total system compressibility, psi^{-1}	1.0288e-4	1.1122e-4	1.1279e-4	9.8079e-5
Layer pressure, psia	4200	4200	4200	4200
Temperature, deg F	350	346	342	339
Gas gravity	0.8600	0.8600	0.8600	0.8600
Water-gas ratio, STB/MMscf	100	50	50	10
Water salinity, ppm	2.0000e4	2.0000e4	2.0000e4	2.0000e4
Gas density, lb/ft^3	12.3831	12.4692	12.5565	12.623
Initial gas viscosity, cp	0.025486	0.0255344	0.0255856	0.0256259
Gas formation volume factor, ft^3/scf	5.3033e-3	5.2667e-3	5.2301e-3	5.2025e-3
Water density, lb/ft^3	57.0574	57.1854	57.3127	57.4078
Water viscosity, cp	0.15772	0.1584	0.15917	0.15983
Water formation volume factor, RB/STB	1.10817	1.10569	1.10324	1.10141
Initial Z-factor	0.97133	0.96942	0.96747	0.966
Initial Gas compressibility, psi^{-1}	1.8025e-4	1.7963e-4	1.7899e-4	1.7850e-4
Water compressibility, psi^{-1}	4.2962e-6	4.2399e-6	4.1845e-6	4.1436e-6

Table 4.5B: Layer boundary data for Case 2.

	Layer 1	Layer 2	Layer 3	Layer 4
Boundary Type	Closed rectangular boundaries	Closed rectangular boundaries	Closed rectangular boundaries	Closed rectangular boundaries
L1, ft	2900	2600	2300	2100
L2, ft	2900	2600	2300	2100
L3, ft	2900	2600	2300	2100
L4, ft	2900	2600	2300	2100
Drainage area, acres	772.2680	620.7530	485.7670	404.9590
Dietz shape factor	30.8815	30.8815	30.8815	30.8815

Table 4.5C: Model parameters for Case 2.

	Layer 1	Layer 2	Layer 3	Layer 4
Model Type	radial homogeneous	radial homogeneous	radial homogeneous	radial homogeneous
Permeability, mD	20.00	30.00	10.00	5.00
Skin factor	0.00	5.00	0.00	0.00
Rate dependent skin coefficient (D), 1/(Mscf/day)	0.00	0.00	0.00	0.00

4.2.2 Production Data

Using the reservoir and fluid parameters from Tables 4.5A through 4.5C, a hypothetical production profile was then input in *PanSystem* in order for the program

to simulate the corresponding flowing bottomhole pressure profile of the reservoir system.

The graph of the production rate and flowing bottom hole pressure over time obtained from the simulation is given in Fig. 4.14. The calibration period which will be used in the history matching is marked in the graph. The calibration period covers the production from 100th day to 383rd day.

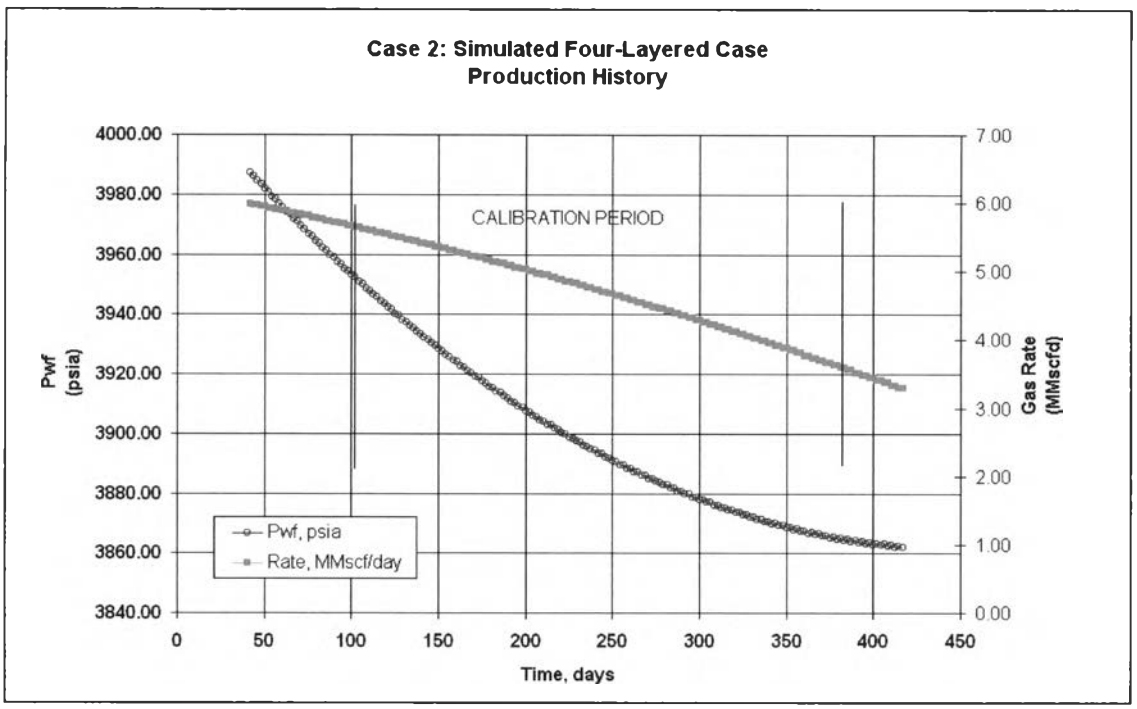

Figure 4.14: Production history for Case 2.

4.2.3 Normalized Pseudo-pressure Tables

The normalized pseudo-pressure tables for Layers 1 through 4 were prepared in a similar manner as in Case 1. The normalized pseudo-pressure tables can be found in the Appendix (see Tables A.2 to A.5). The corresponding normalized pseudo-pressure graphs are also in the Appendix (see Figs. A.2 to A.5).

From the normalized pseudo-pressure tables, the flowing bottomhole pressures were calculated. The graph of the production rate and the flowing bottom hole pressure in terms of normalized pseudo-pressures is given in Fig. 4.15. Note that the flowing bottomhole pressures (in terms of normalized pseudo-pressures) over time are very similar for all the layers. This is because *PanSystem* assumes that each layer has the same flowing bottomhole pressure.

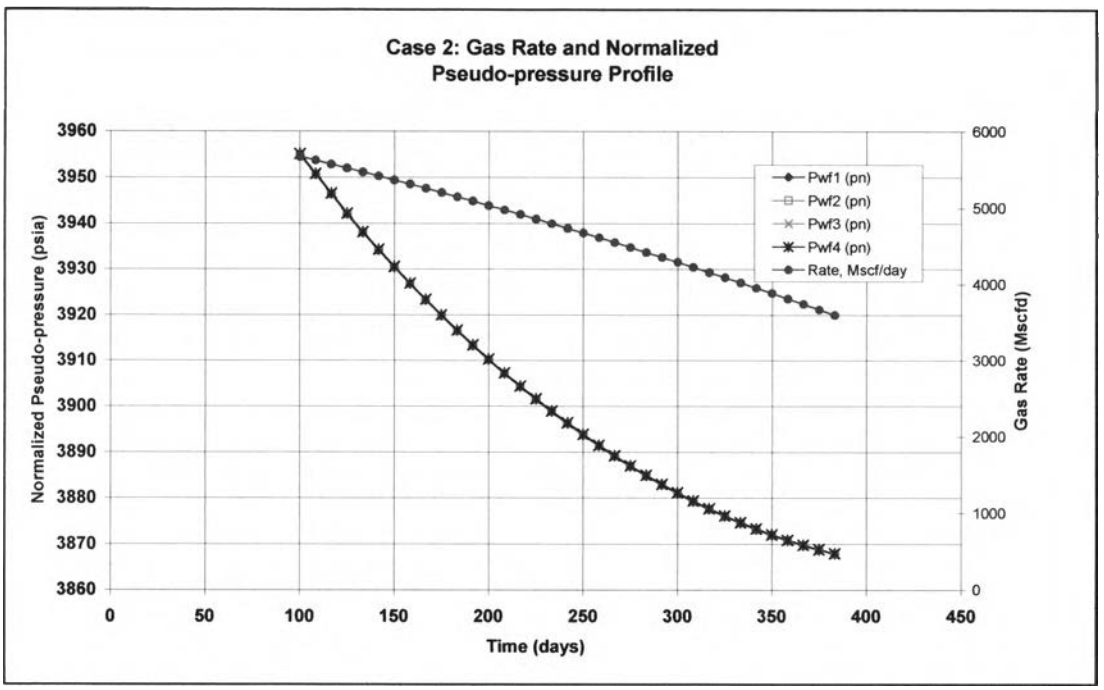

Figure 4.15: Plot of gas rate and normalized pseudo-pressures (Case 2).

4.2.4 History Matching

History matching using the LSFM program was a lot simpler in this case as the OGIP and the predicted gas rate contribution from each layer from the *PanSystem* were used as the basis for the initial guesses of G, J_g and G_p' of each layer.

4.2.5 Results and Discussion

The result of the history matching is given in Fig. 4.16. The comparison of the OGIP from the LSFM program and PanSystem is given in Table 4.6.

Table 4.6: OGIP comparison for Case 2.

	LSFM Program OGIP (bscf)	PanSystem OGIP (bscf)	% Difference
Layer 1	15.6001	15.4671	0.85
Layer 2	6.7352	6.6950	0.59
Layer 3	13.9951	13.9010	0.67
Layer 4	6.9200	6.9082	0.17

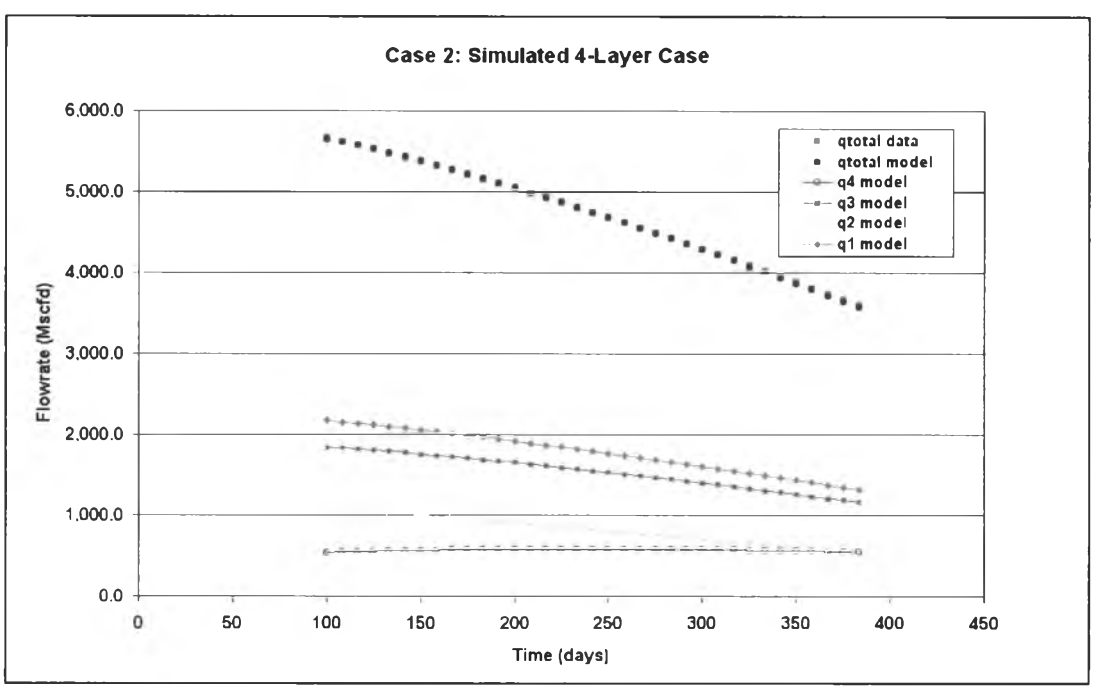

Figure 4.16: History matching result for Case 2.

Examination of Figure 4.16 reveals that Layer 1 and Layer 3 are the main contributors to the total production of this well. Inspection of the layer properties of the four sands shows that Layer 1 has the highest permeability thickness (400 mD-ft).

Although Layer 2 and Layer 3 has the same permeability-thickness value of 300 mD-ft, the existence of skin in Layer 2 caused a lower flow contribution from this layer.

It is worthwhile to note that the depletion trend in Layer 1 through 3 follows a similar pattern. This is not the case for Layer 4. Layer 4 is producing at a constant and at a much-reduced rate compared to the other three layers. This could have been attributed to the low permeability of this sand.

Table 4.6 shows the comparison of the OGIP calculated by the LSFM program and the *PanSystem* Program for each layer. The OGIP values calculated by *PanSystem* seem to be slightly higher than what the LSFM Program predicts. Again, the close results obtained from the LSFM program and *PanSystem* allows us to conclude that the LSFM program is setup correctly and can be used for predicting OGIP.

4.3 Case 3: Simulated Four-Layered Reservoir with Different Initial Reservoir Pressures

Case 3 is a simulated case that intends to investigate the applicability of the LSFM Program in predicting OGIP for commingled reservoirs whose layers have different initial reservoir pressures. This case is analyzed because most, if not all, of commingled reservoirs have unequal initial layer pressures.

Case 3 is a duplicate of Case 2 except that the initial reservoir pressures are varied for each layer. Table 4.7 provides the initial reservoir pressure values of the four layers.

Table 4.7: Initial reservoir pressure values for each layer for Case 3.

	Layer 1	Layer 2	Layer 3	Layer 4
Initial reservoir pressure, psia	4200	4150	4100	4000

For this case, the OGIP's calculated from the LSFM Program are expected to be the same for layer 1 but different for layers 2 to 4 due to the change in the initial layer pressures. The total gas rate is expected to remain unchanged but the production from each sand should be different as a consequence of the differences in the initial reservoir pressures of the layers. Performing the LSFM modeling will enable us to know the effect of having different initial reservoir pressures on the relative contribution of each sand to the total production of the well.

4.3.1 Production Data and Normalized Pseudo-pressures

The total production profile for Case 3 is the same as that of Case 2. However, the flowing bottomhole pressures calculated by the *PanSystem* program are different as a result of the unequal initial reservoir pressures of the layers. The normalized pseudo-pressure tables for Case 2 were used for calculating the normalized pseudo-pressures. The graph of the production rate and the flowing bottom hole pressure in terms of normalized pseudo-pressures is given in Fig. 4.17. Note that the flowing bottomhole pressure profile for each layer are slightly different in this case as compared to Case 2 where the bottomhole pressure profiles are almost the same.

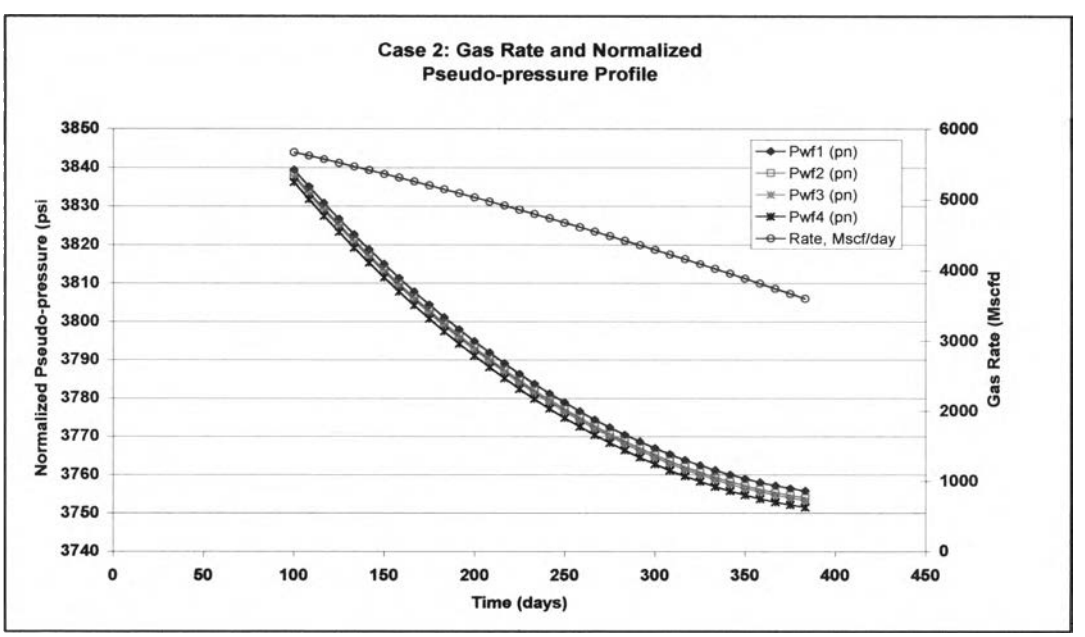

Figure 4.17: Plot of gas rate and normalized pseudo-pressures (Case 3).

4.3.2 History Matching

The same calibration period and convergence criteria used in Case 2 were applied in the history matching for Case 3.

The plot of the history matching using the LSFM Program is given in Fig. 4.18. The comparison of the history matching for Case 2 and Case 3 is provided in Table 4.8. It also provides the OGIP values from *PanSystem* for comparison. The comparison of the production rates and the calculated gas flow coefficients for Case 2 and Case 3 is given in Table 4.9.

Table 4.8: Comparison of OGIP from LSFM (Case 2 and Case 3) and *PanSystem*.

	LSFM - Case 2 OGIP (bscf)	PanSystem-Case 2 OGIP (bscf)	LSFM - Case 3 OGIP (bscf)	PanSystem-Case 3 OGIP (bscf)
Layer 1	15.6001	15.4671	15.6001	15.4671
Layer 2	6.7352	6.6950	6.611	6.6346
Layer 3	13.9951	13.9010	13.622	13.6495
Layer 4	6.9200	6.9082	6.636	6.6562

Table 4.9: Comparison of the production rate profile and J_g for Case 2 and Case 3.

	kh (mD-ft)	Production Rate (Mscfd) from start to end of Calibration Period		Gas Flow Coefficient J_g (scf/psi-d)	
		Case 2	Case 3	Case 2	Case 3
Layer 1	400	2,171 to 1,317	2840 to 1665	9,960.2	9,960.0
Layer 2	300	1,095 to 543	1,076 to 573	5,645.1	5,645.0
Layer 3	300	1,841 to 1,162	1,354 to 1,057	8,500.2	8,500.0
Layer 4	75	539 to 546	207 to 311	2,490.4	2,489.9

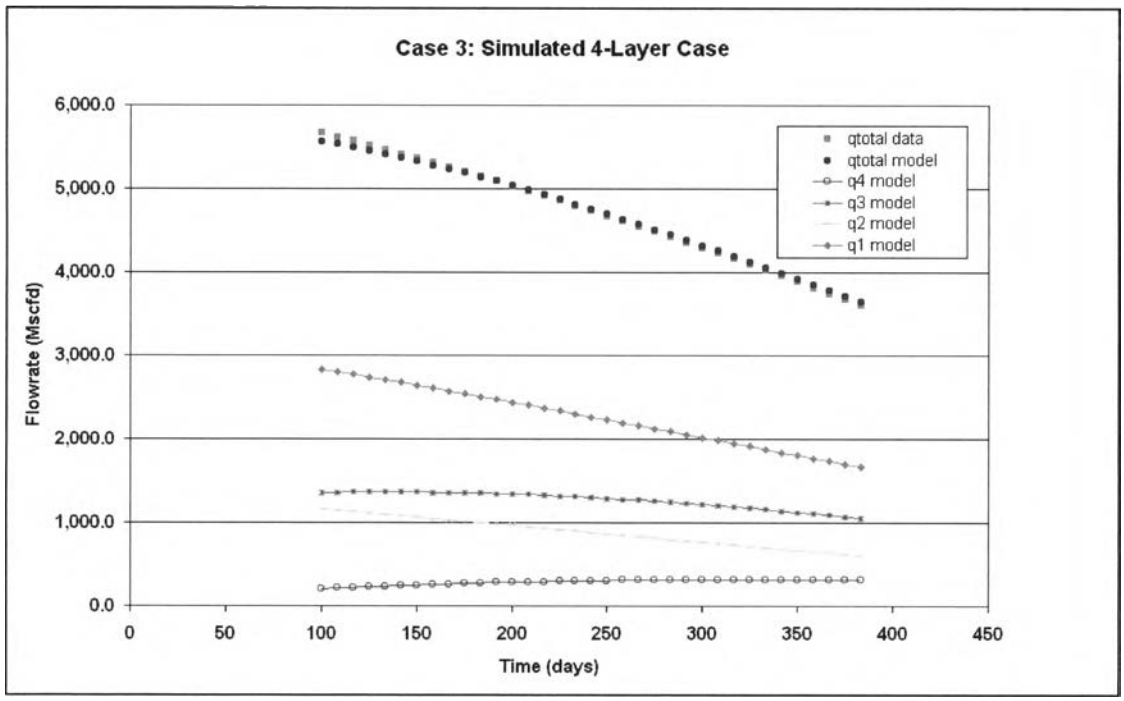

Figure 4.18: History matching result for Case 3.

4.3.3 Discussion of Results

From Table 4.8, both *PanSystem* and LSFM showed lower OGIP values for layers 2 to 4 where the initial reservoir pressures were lower compared to those of Case 2. Layer 1, having the same initial reservoir pressure as in Case 2, showed the same OGIP.

The total system flowrate remained the same as in Case 2 however, the relative contribution of each layer did change as a result of the differences in the initial layer pressures. Examination of Table 4.9 reveals that there is a significant increase in the production of Layer 1, the layer with the highest initial pressure. Conversely, the other 3 layers showed a decrease in production.

The change in the relative contribution from each layer is the most distinctive effect of the differences in the initial pressures of the layers. In Case 3, having different initial reservoir pressures resulted to a different flowing bottomhole pressure

profile. Comparison of Fig. 4.15 and 4.17 shows that the flowing bottomhole pressures of the sands in Case 3 are lower than that of Case 2.

The difference in the flowing bottomhole pressure for Case 2 and Case 3 and the difference in the initial reservoir pressures of the layers both affect the pressure drawdown for each layer. Pressure drawdown is defined as the difference between the static reservoir pressure and the flowing bottomhole pressure of the layer. Therefore, the drawdown of each layer in Case 3 will be different from that of Case 2 depending on the values of the layer pressures and the layer flowing bottomhole pressures.

The increased production in Layer 1 can be explained by the increase in pressure drawdown in Layer 1. Although the initial reservoir pressure in Layer 1 for Case 2 and Case 3 are the same (4200 psia), the lower flowing bottomhole pressure resulted in an increase pressure drawdown for this layer, hence, the increased production in Layer 1.

However, this was not the case for the other three layers in Case 3 because the initial reservoir pressures in these layers are all lower than that of Case 2 (refer to Table 4.7 for the initial pressure values of the layers). Although the flowing bottomhole pressures of all the sands were smaller compared to Case 2, the lower initial layer pressures decreased the pressure drawdown in Layers 2 to 4, resulting in the decrease in the relative contribution from these layers.

The understanding from this simulation case will be of great importance in evaluating the production trend of the layers from actual field cases where the layers are at different pressures.

4.4 Actual Field Cases

To test the capability of the LSFM program for predicting gas in place on actual field cases, two gas wells in the Gulf of Thailand were investigated. Actual well and reservoir information and field production data were used in these cases. The producing well pressures through time are assumed to be known for the entire history of the well and are used in the model calculations.

Two cases were studied: the first case is a two-layered reservoir model and the second one, a four-layered reservoir model.

4.5 Case 4: Two-Layered Reservoir with Different Initial Reservoir Pressures

4.5.1 Reservoir and Fluid Properties

Case 4 is an investigation of a well producing from a two-layered commingled reservoir with different initial reservoir pressures. For confidentiality, the original well name is withheld. For the purpose of this research paper, the well will be labeled as Well #1. The reservoir and fluid properties of this well are given in Table 4.10.

Table 4.10 shows that both sands from this commingled reservoir system have roughly the same moderate porosities and permeability values. The thicknesses of the sands are small which is typical of the compartmentalized reservoirs in the Gulf of Thailand. The two sands are at different initial reservoir pressures, with the difference being 573 psi. Layer 1 and Layer 2 are at 7830 ft and 7358 ft TVD subsea, respectively. The schematic diagram of the well completion is given in Fig. 4.19.

Table 4.10: Reservoir and fluid property data for Case 4.

Properties	Layer 1 (78-3)	Layer 2 (73-6)
Layer thickness, ft	10	15
Porosity, fraction	0.21	0.20
Water saturation, fraction	0.54	0.41
Permeability*, mD	53.5	37.8
Gas gravity	0.87	0.87
Initial pressure, psig	3990	3417
Temperature, deg F	318	307

*correlated from permeability-porosity cross plot, UNOCAL empirical equation

4.5.2 Production Data

Well #1 started production on 16-March-2001 after perforation of two sands (sand 73-6 and sand 78-3). Table A.6 (see Appendix) provides the well test data from 16-March-2001 through 22-June-2003. The well test data provides the information on when the well test was performed, the flowing tubing head pressure of the well, the choke opening, and the flowrates of gas, water and condensate. The duration of the well test is also provided in the table. The production rate and the flowing tubing head pressure profiles of the well are given in Fig. 4.20.

Another useful data for interpreting the production history of the well is the well status report. This report provides the daily status of the well and indicates whether the well is producing or is shut-in. If the well is on production, it provides the flowing tubing head pressure and the choke setting at which the well is flowing. If the well is shut-in, it provides the shut-in pressure and the duration at which the well is off-line. Table A.7 in the Appendix provides the status report of Well #1.

The well status report must be used in conjunction with the well test data to determine the actual flow period and shut-in (off-line) periods of the well. It is

important to account for periods at which the well is shut-in particularly in the calculation of the cumulative production. Otherwise, the cumulative production will be overestimated, resulting in a serious error in the history matching.

After reconciling the well status report and the well test data, the periods at which the well is off-line were taken out from the flow period of the well.

Using actual field production data requires careful pre-processing and analysis in order to make them useful and reliable. For one, actual data are often times predisposed to measurement inaccuracies. These measurement inaccuracies will lead to erroneous model rates and as a consequence will result in a poor match.

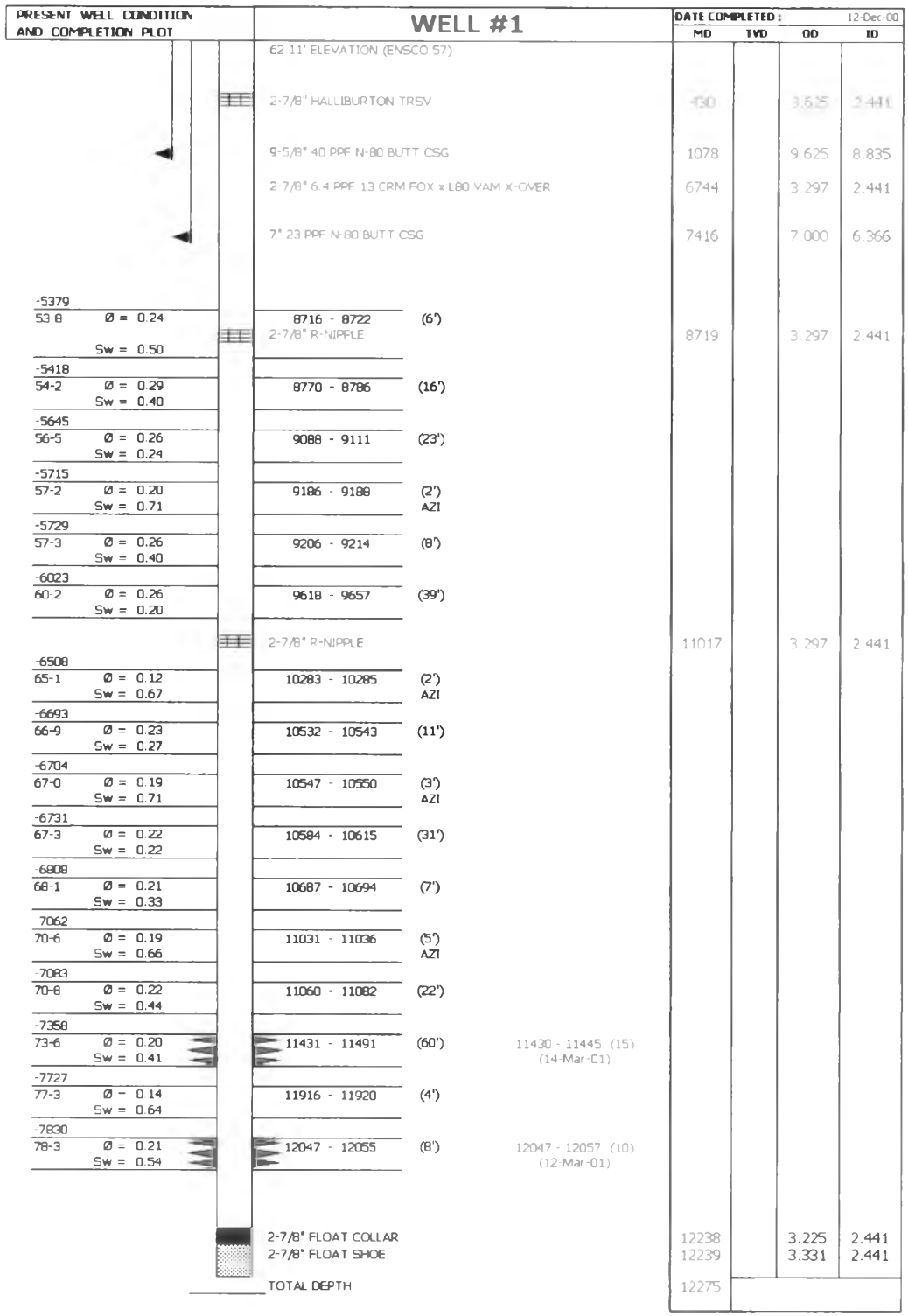

Figure 4.19: Well #1 schematic diagram (Case 4).

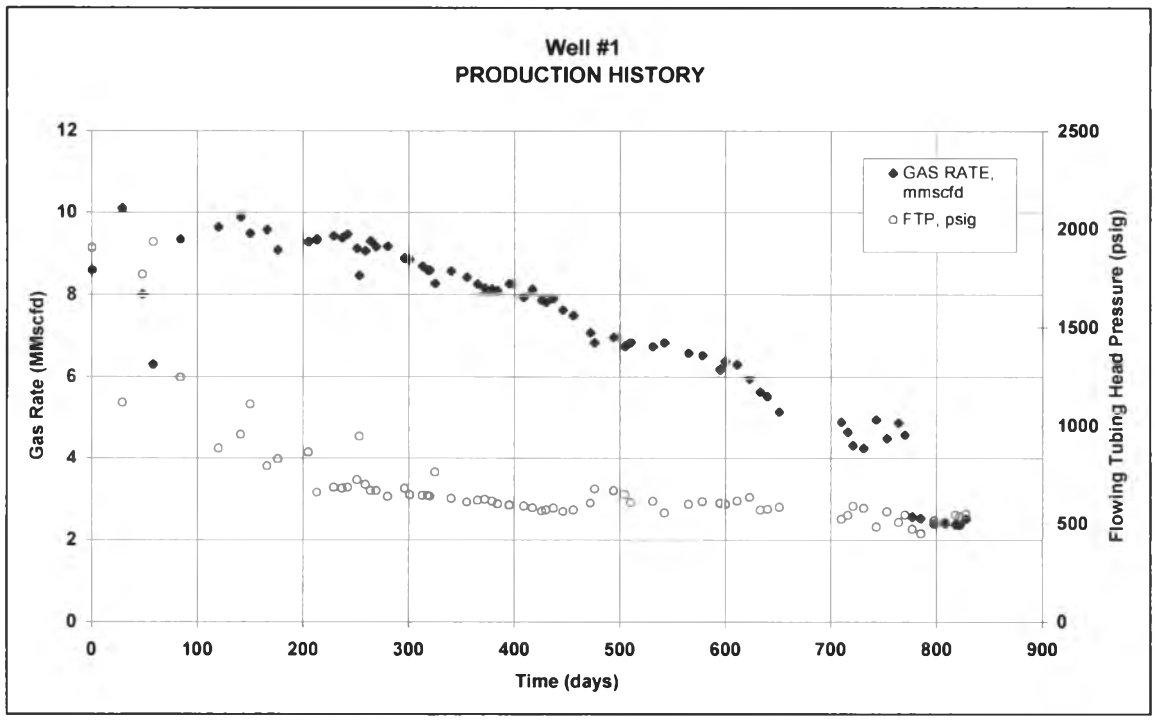

Figure 4.20: Gas rate and flowing tubing head pressure for Well #1 (Case 4).

4.5.3 Flowing Bottomhole Pressures

The flowing tubing head pressures from the well test data have to be converted to flowing bottomhole pressures in order to use it in the LSFM Program. Calculation of the flowing bottomhole pressures was done using the *Petroleum Experts Prosper Suite*[16]. The multi-phase flow correlation used was the Duns and Ros Correlation. This correlation was selected as it usually performs well for gas-condensate wells having mist flow.

Accurate calculation of flowing bottomhole pressures not only requires a suitable multi-phase flow correlation but also a good measurement of the tubing head pressure, temperature and surface flowrates of the gas, water and condensate. The well test data that have been often in question are the condensate and water rates. This is because well testing is typically carried out with a two-phase separator where there is no true separation of the liquid phases (water and condensate). Having incorrect

condensate and water rates normally leads to inaccurate calculation of the bottomhole pressures.

Therefore, after calculating the bottomhole pressures from *Prosper*, careful attention was given to those data points with abnormally high or low bottomhole pressures. For those suspicious data points, the bottomhole pressure of the previous or the succeeding well test was used as long as the well test interval was fairly close.

The calculated bottomhole pressures together with the gas rates are presented in Fig. 4.21.

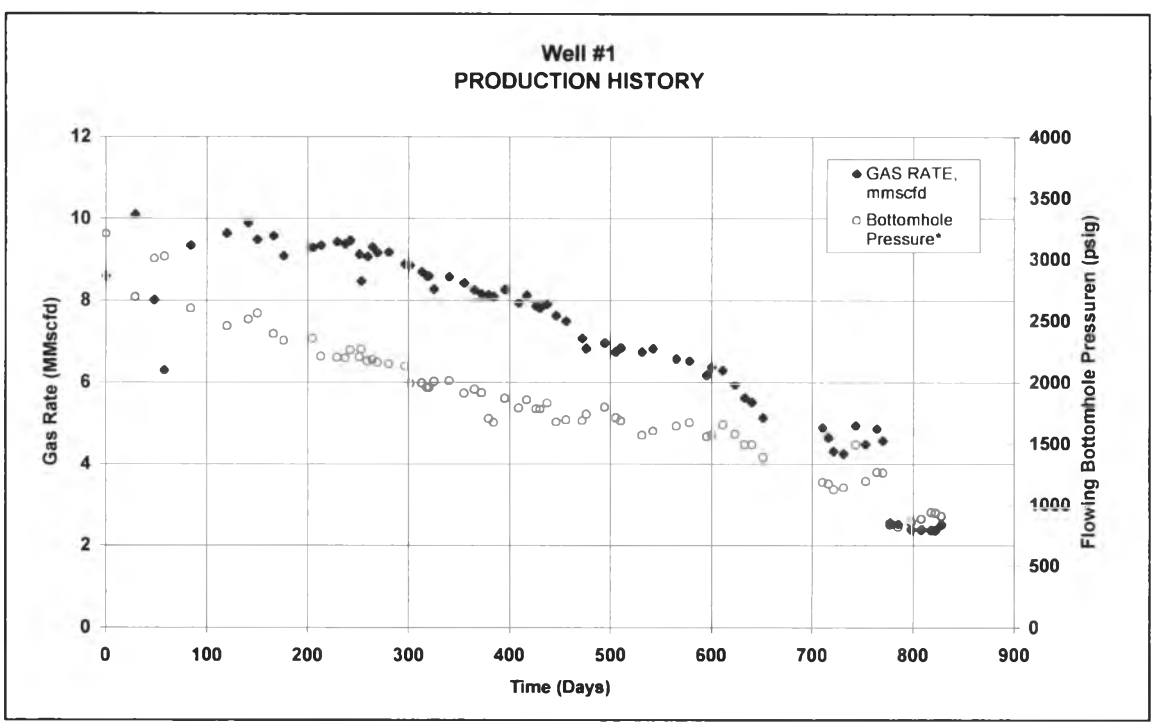

Figure 4.21: Calculated bottomhole pressures from PetEx Prosper program for Well #1 (Case 4).

4.5.4 Normalized Pseudopressures

The normalized pseudo-pressure tables and graphs are presented in Tables A.8 to A.9 and Figs. A.6 to A.7 (see Appendix).

4.5.5 History Matching

As discussed previously, making the most reasonable initial guesses for G_k, J_{gk} and G_{pk}' is very important in order to make the LSFM program converge to the correct minimum. Again, different combinations of initial guesses of the unknown parameters can be made to fit the model rate equation to the actual rate data. In order to make the most accurate initial guesses for the parameters, the following considerations were done:

1. The *kh* values of Layer 1 and Layer 2 were compared. From Table 4.11, the *kh* values of Layer 1 and Layer 2 can be calculated and are 535 mD-ft and 567 mD-ft, respectively. These values are very close, so we would expect to have roughly equal contribution from the two layers if and only if they are producing against the same reservoir pressure. However, this is not the case since Layer 1 was producing at a higher reservoir pressure than Layer 2. It is then expected that the main production was initially coming from Layer 1 which means that a higher initial cumulative production could be allocated to Layer 1.

2. Since the *kh* of the two layers are comparable to each other, the initial guesses for the gas productivity index for both layers were made as close as possible.

3. Several combinations of guesses for G, J_g and G_p' for each layer were made while keeping in mind the earlier considerations mentioned. For each combination, the plot of the model rate equation and the actual rate data are "visually matched". Once a satisfactory visual match is obtained, these are then considered as the initial guesses for G, J_g and G_p' of each layer which were then used for the actual history matching.

The calibration period used for the history matching was from 29-Aug-01 to 15-Oct-02. The result of the history matching is presented in Fig. 4.22. The calculated OGIP and gas flow coefficients are given in Table 4.11.

Table 4.11: Calculated OGIP and J_g for Case 4.

	OGIP (bscf)	Gas Flow Coefficient (scf/psi-d)
Layer 1 (78-3 sand)	8.853	6116.58
Layer 2 (73-6 sand)	5.581	7025.61

4.5.6 Discussion of Results

Fig. 4.22 shows the match of the total actual rate and the total model rate from the LSFM program. As evident in the graph, there is a lot of data scatter from the model rate compared to the simulated cases earlier investigated. This is true for actual field cases where a perfect match is rarely achieved due to the measurement inaccuracies as explained earlier.

Inspection of the layer rates (see Fig. 4.22) shows that Layer 1 was the main producer in this well, providing about 60% to the total production. Both layers were declining at almost the same rate as evident in the comparable values of the gas flow coefficient J_g.

The predicted OGIP shows that Layer 1 has a higher gas in place than Layer 2.

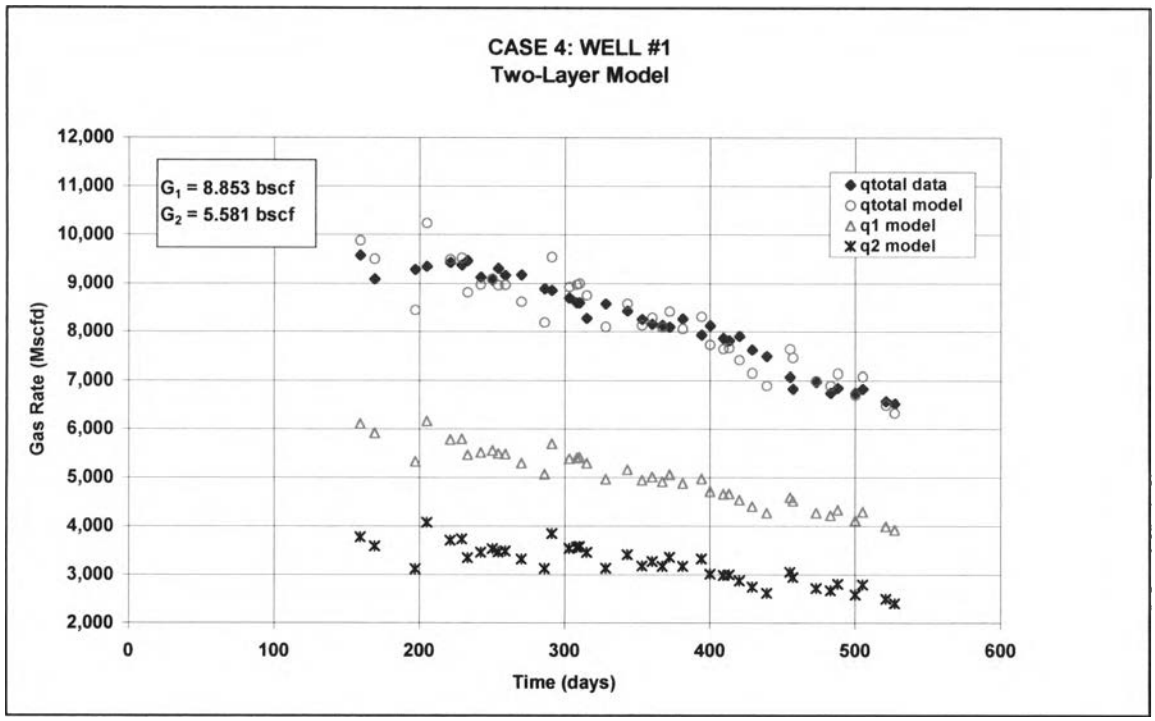

Figure 4.22: LSFM history matching result for Case 4.

4.5.7 Comparison of OGIP with the Commingled Wellbore Model

The Commingled Wellbore Model (CWM) developed by Nick Last, UNOCAL Consultant, was also run on Case 4 using the same well and reservoir parameters and production history used in the LSFM Model.

As mentioned in Chapter 2, the CWM calculates the OGIP value using volumetric equation. The OGIP is a function of reservoir pressure, layer thickness, porosity, water saturation, temperature and area. The CWM assumes that all the above parameters are known except for the area. Thus, the CWM estimates the area and uses this area to generate a production history of the well over time that matches the actual production history (flowing pressures and production rate over time) of the well.

The results from the CWM is provided in Table 4.12. The results include the drainage area that were input in the model for the calculation of the OGIP values that

match the production and flowing wellhead pressure history of the well. The plot of the history match using the CWM is presented in Fig. 4.23.

Table 4.12: OGIP and drainage areas calculated from the CWM for Case 4

Layer	OGIP (bscf)	Drainage area (acres)
Layer 1 (78-3 sand)	8.870	2280
Layer 2 (73-6 sand)	5.600	178

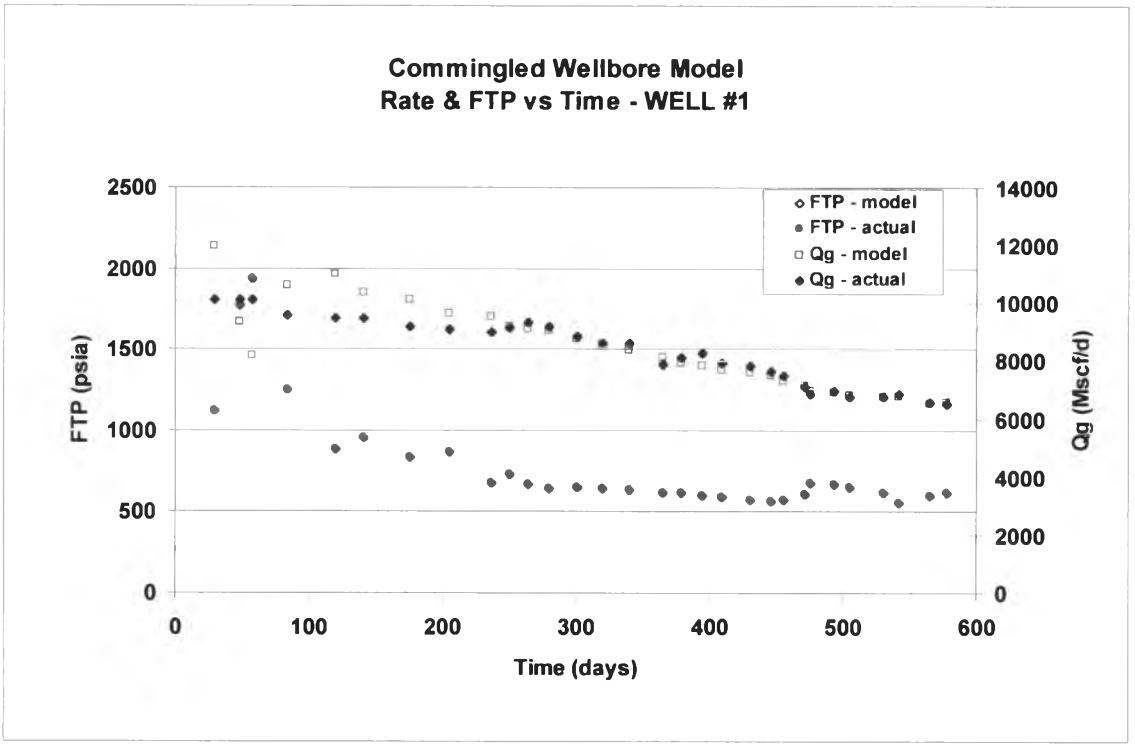

Figure 4.23: CWM history matching result for Case 4.

The comparison of the OGIP values from the LSFM and the CWM is presented in Table 4.13.

Table 4.13: Comparison of the OGIP values between LSFM and CWM for Case 4.

	LSFM Program OGIP (bscf)	CWM OGIP (bscf)	% Difference
Layer 1	8.853	8.870	0.189
Layer 2	5.581	5.600	0.323

Table 4.13 shows a close match of the OGIP values from the LSFM and CWM. The CWM is predicting the OGIP slightly higher than the LSFM.

4.5.8 Sensitivity Analysis

Three sensitivity analysis runs were made in order to see how the calculated OGIP values vary when some input parameters are changed. The first sensitivity run investigates the effect of data filtering in the history matching. In this run, only model rate data points that closely match the actual rate data from the original run were used in the non-linear regression analysis.

The second and third runs examine the sensitivity of the OGIP values predicted by the LSFM with the multi-phase correlation used in the calculation of the bottomhole pressures. As mentioned earlier, the correlation used in Case 4 was the Duns and Ros Correlation. For the sensitivity runs, the Petroleum Experts 4 and Gray Correlations were used. These were the recommended correlations as they are the most applicable to the fluid type and flow regime of the case being investigated. The Petroleum Experts 4 Correlation is an advanced mechanistic model for any angled well suitable for any fluid (including retrograde condensates). The Gray Correlation, on the other hand, gives good results in gas wells for condensate ratios up to around 50 bbl/mmscf and high produced water ratios.

The history matching for the sensitivity runs are presented in Figs. 4.24 to 4.26. The comparison of the OGIP values is given in Table 4.14.

Table 4.14: Comparison of the OGIP values for Case 4 (original and sensitivity runs).

	OGIP VALUES (bscf)			
	Original Run	Sensitivity Run 1	Sensitivity Run 2	Sensitivity Run 3
Layer 1	8.853	8.851	10.099	8.921
Layer 2	5.581	5.611	7.098	5.572

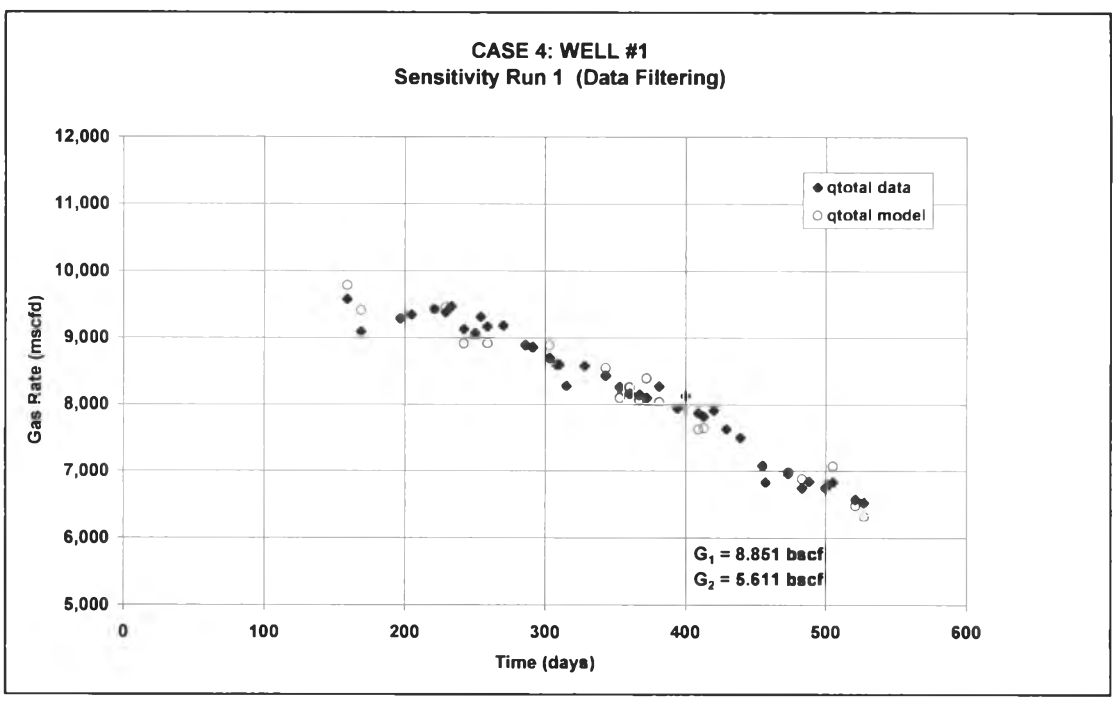

Figure 4.24: History matching result for sensitivity run 1 (Case 4).

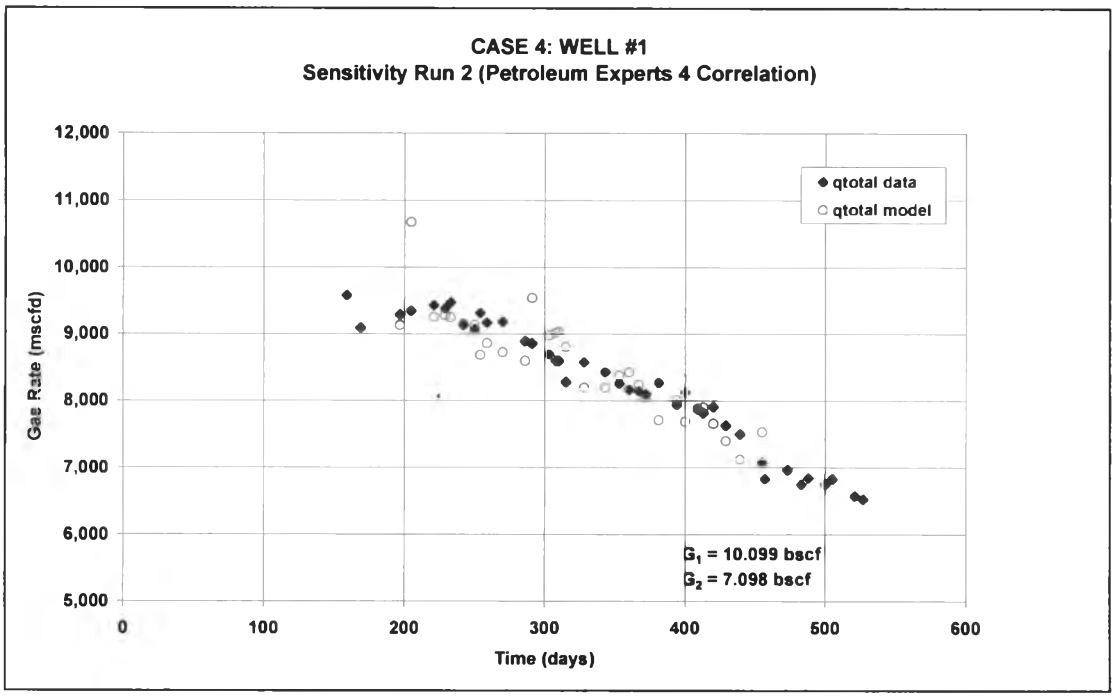

Figure 4.25: History matching result for sensitivity run 2 (Case 4).

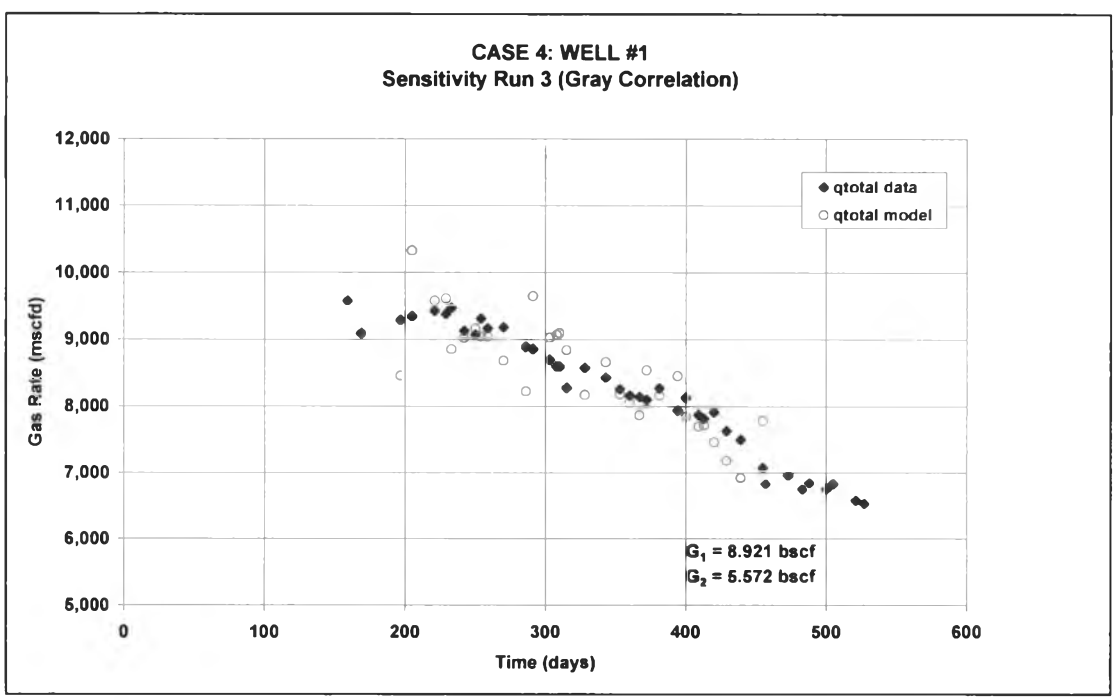

Figure 4.26: History matching result for sensitivity run 3 (Case 4).

A better match with the Gauss-Marquardt Algorithm was obtained when data filtering was applied in Sensitivity Run 1. The comparison of the convergence criteria with the original run is shown Table 4.15. From Table 4.15, the history match was achieved with a considerably lower convergence criteria. Although improvement in the convergence was achieved, it is worthwhile to note though that the values of the OGIP did not change much.

From the results of sensitivity runs 2 and 3, it is evident that the choice of the multi-phase correlation affects the predicted OGIP. For this particular case, the use of Petroleum Experts 4 Correlation for the bottomhole calculation overpredicts the OGIP while the Gray Correlation seems to show a comparable OGIP value as the Duns and Ros Correlation. The Petroleum Experts 4 Correlation calculates lower bottomhole pressures which then requires higher G, J_g and G_p' from each layer to make the model production rate match the actual rate data. Therefore, care should be used in choosing the correlation to use for the bottomhole pressure calculation. There is no universal rule for selecting the best flow correlation so it is recommended that correlation comparison always be carried out. For best results, pressure gradient plots generated by the program should be compared with actual measured gradient survey data. Unfortunately, this well does not have any pressure gradient survey done to date so we have to rely on the simulated bottomhole pressures calculated by the program.

Table 4.15: Comparison of convergence criteria:
original and sensitivity runs (Case 4).

	Case 4 Original Run		Sensitivity Run 1	
	Layer 1	Layer 2	Layer 1	Layer 2
dG	0.5	0.5	0.5	0.5
dJ_g	0.8	0.8	0.3	0.3
dG_p'	0.2	0.2	0.1	0.1

4.6 Case 5: Four-Layered Reservoir with Different Initial Reservoir Pressures

Case 5 investigates the application of the LSFM in a four-layered commingled gas reservoir with different initial reservoir pressures. As in Case 4, the real name of the well under study will be withheld and will only be labeled as Well #2.

4.6.1 Reservoir and Fluid Properties

The reservoir and fluid properties of this well are provided in Table 4.16.

Table 4.16: Reservoir and fluid property data for Case 5.

Properties	Layer 1 (78-6)	Layer 2 (77-8)	Layer 3 (75-8)	Layer 4 (73-7)
Layer thickness, ft	15	6	13	17
Porosity, fraction	0.15	0.20	0.17	0.26
Water saturation, fraction	0.45	0.49	0.40	0.36
Permeability*, mD	6.7	37.8	13.4	302
Gas gravity	0.86	0.86	0.86	0.86
Initial pressure, psig	3682	3643	3560	3427
Temperature, deg F	319	317	312	310

*correlated from permeability-porosity cross plot, UNOCAL empirical equation

Unlike Case 4, there is a pronounced permeability-thickness contrast among the four layers. However, the initial layer pressures do not show much disparity as the sands are close to each other except for Layer 4. The schematic diagram of the well is provided in Fig. 4.27.

4.6.2 Production Data

Production from Well #2 commenced on 22-Mar-2001 when the 78-6 sand was perforated. Sands 77-8, 75-8 and 73-7 were then perforated a month after. The well test data and the well status report are presented in Table A.10 and Table A.11, respectively (see Appendix). As was done in Case 4, the period at which the well was offline was removed from the flow period of the well. The measured gas rate and flowing tubing head pressure over time are presented in Fig. 4.28.

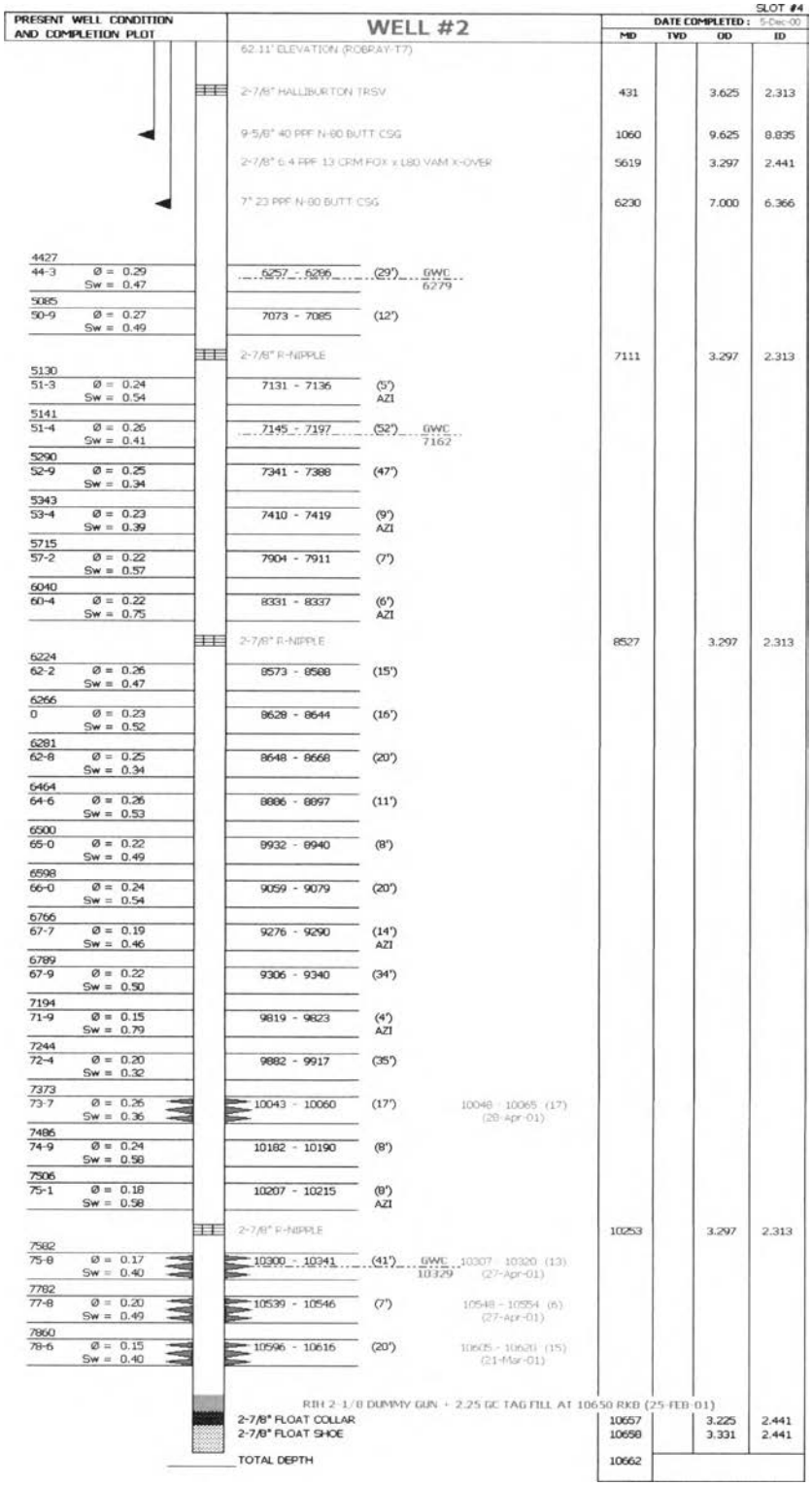

Figure 4.27: Well #2 schematic diagram (Case 5).

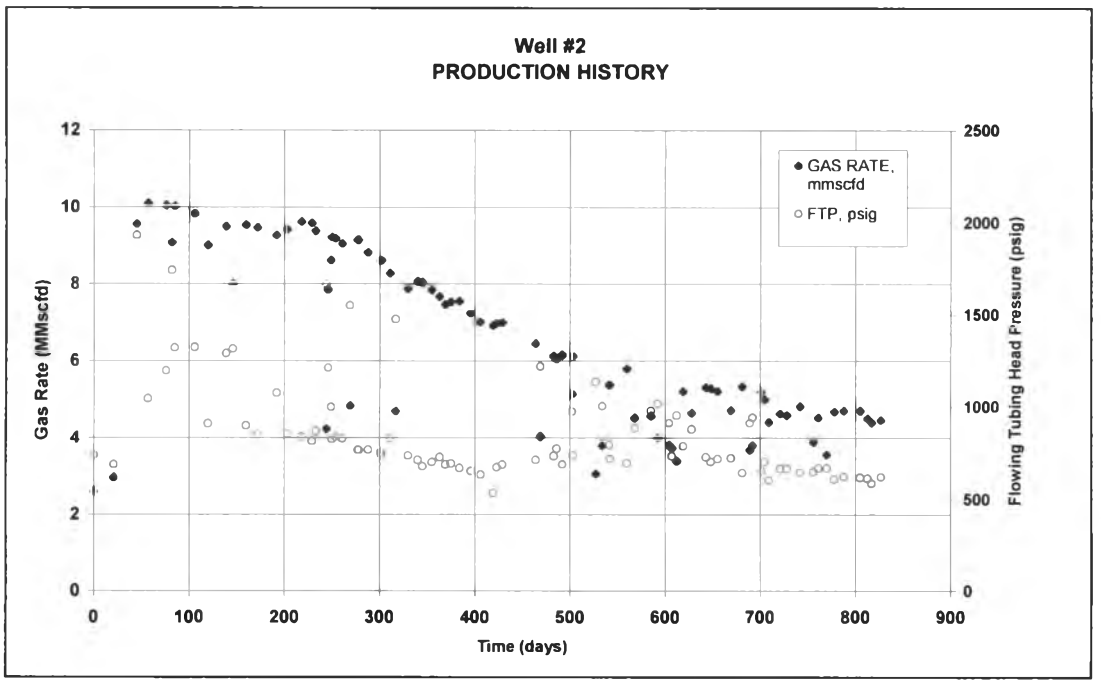

Figure 4.28: Gas rate and flowing tubing head pressure for Well #2 (Case 5).

4.6.3 Flowing Bottomhole Pressures

The flowing bottomhole pressure for this case was also calculated using Prosper with the Duns and Ros Correlation. The plot of the flowing bottomhole pressure over time is given in Fig. 4.29.

4.6.4 Normalized Pseudopressures

The normalized pseudo-pressure tables and graphs are presented in Tables A.12 to A.15 and Figures A.8 to A.11, respectively.

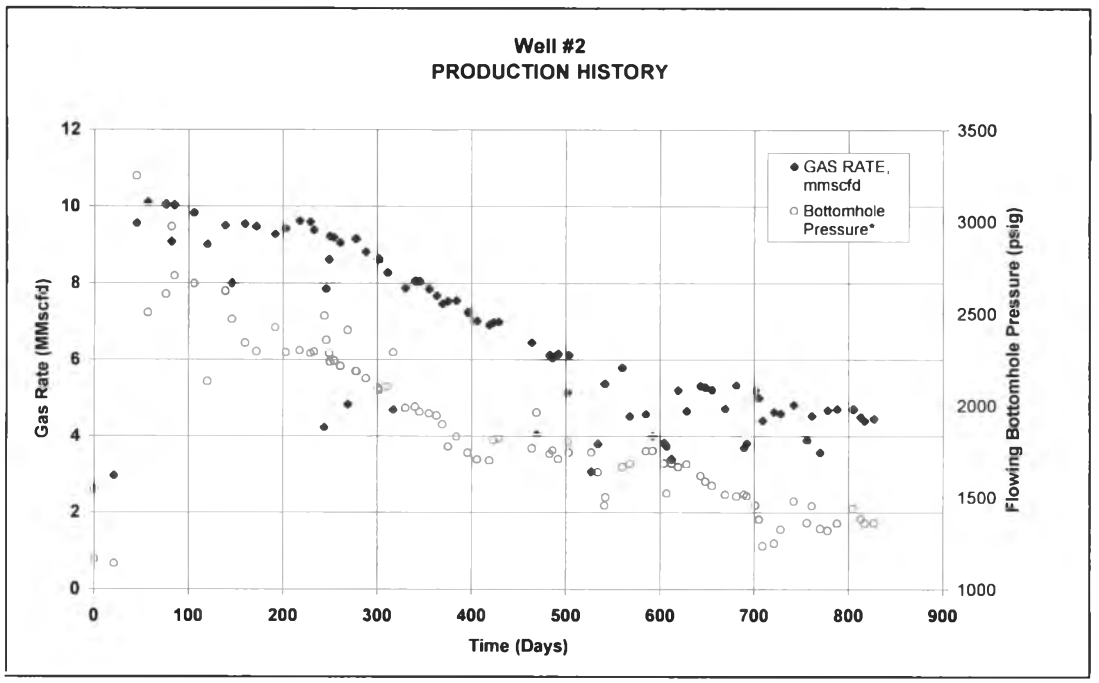

Figure 4.29: Calculated bottomhole pressures from PetEx Prosper program for Well #2 (Case 5).

4.6.5 History Matching

The same considerations were made in making the initial guesses for the layer parameters G_k, J_{gk} and G_{pk}'. The *kh* values and the initial reservoir pressures of the four sands were compared in order to provide a good initial prediction of which layers are contributing mainly to the total production. Since there is not much difference in the layer pressures, it follows that the main contribution should be coming from Layers 4 as it has the highest *kh* among the sands. The same "graphical matching" technique was applied until the most suitable combination of G_k, J_{gk} and G_{pk}' was used as the final initial guesses for the history matching. The calibration period for the history match was from 01-Dec-01 to 17-Jun-03.

The history matching result for Case 5 is presented in Fig. 4.30. The calculated OGIP and gas flow coefficients are given in Table 4.17.

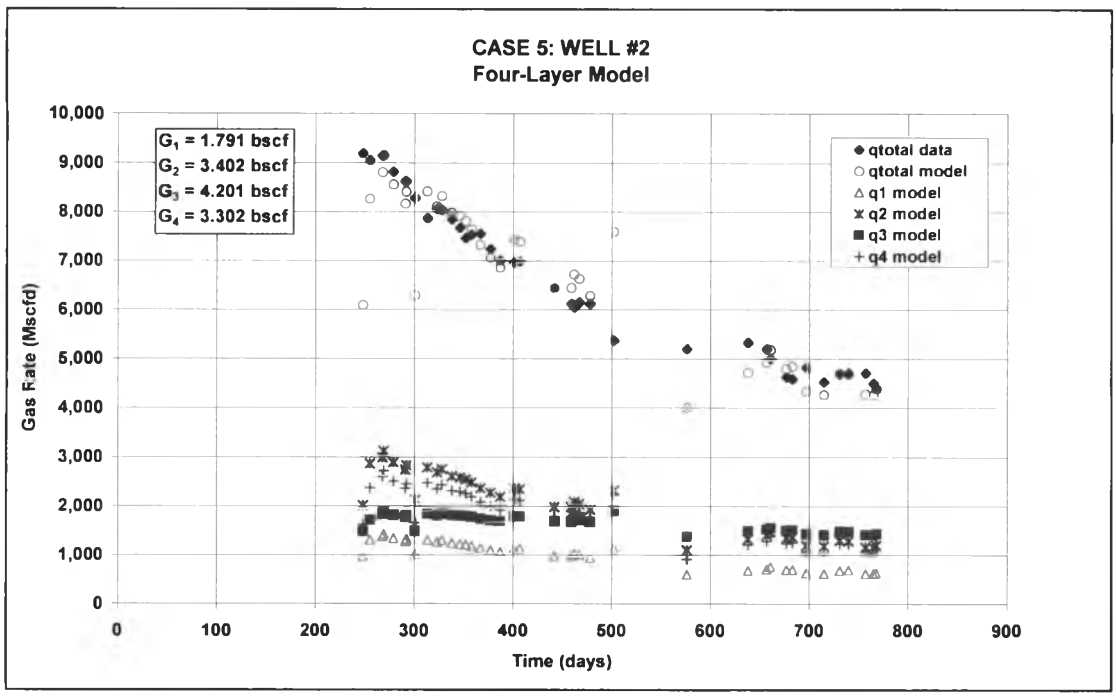

Figure 4.30: LSFM history matching result for Case 5.

Table 4.17: Calculated OGIP and Jg for Case 5.

	OGIP (bscf)	Gas Flow Coefficient (scf/psi-d)
Layer 1 (78-6 sand)	1.791	1448.19
Layer 2 (77-8 sand)	3.402	3348.41
Layer 3 (75-8 sand)	4.201	1601.26
Layer 4 (73-7 sand)	3.302	3858.32

4.6.6 Comparison of OGIP with the Commingled Wellbore Model

The result of the history matching with the CWM is presented in Fig. 4.31. The OGIP and drainage areas calculated from the CWM are provided in Table 4.18. The comparison of the OGIP values btween the LSFM and CWM is given in Table 4.19.

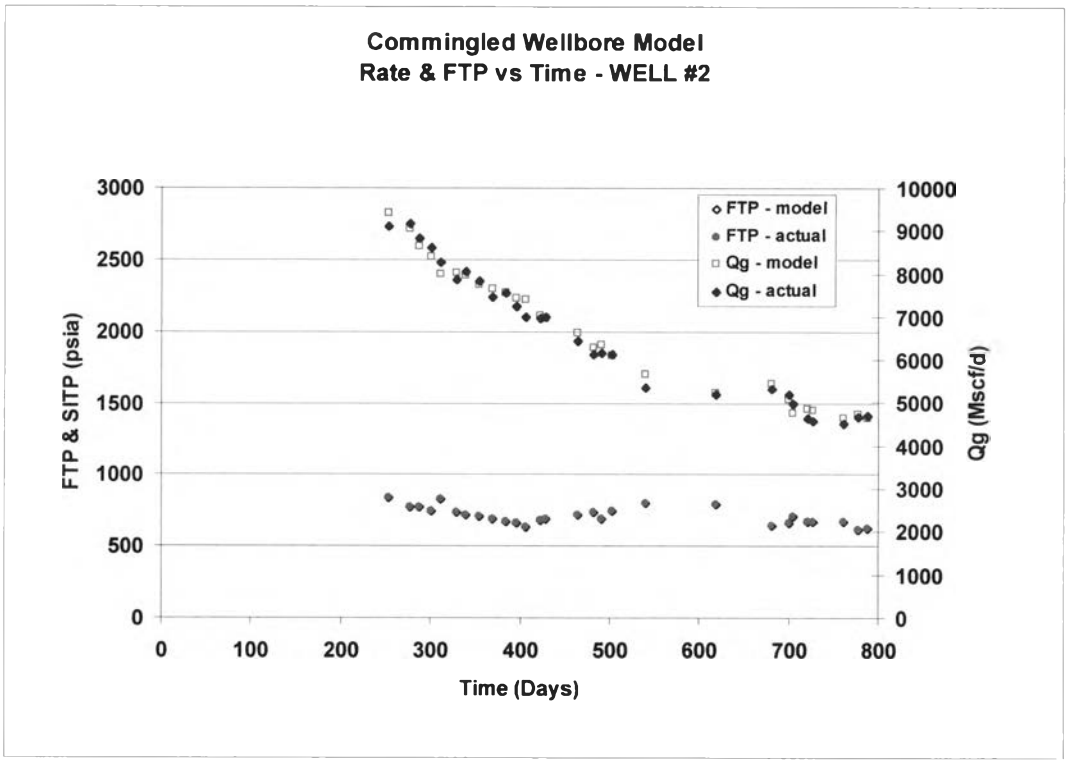

Figure 4.31: CWM history matching result for Case 5.

Table 4.18: OGIP and drainage areas calculated from the CWM for Case 5

Layer	OGIP (bscf)	Drainage area (acres)
Layer 1 (78-6 sand)	1.740	192
Layer 2 (77-8 sand)	3.350	737
Layer 3 (75-8 sand)	4.140	428
Layer 4 (73-7 sand)	3.220	173

Table 4.19: Comparison of the OGIP Values between LSFM and CWM (Case 5):

	LSFM Program OGIP (bscf)	CWM OGIP (bscf)	% Difference
Layer 1	1.791	1.740	2.48
Layer 2	3.402	3.350	1.45
Layer 3	4.201	4.140	1.53
Layer 4	3.302	3.220	2.85

4.6.7 Discussion of Results

From Fig. 4.23, it seems that a better match was obtained for Case 5 than for Case 4 except for some data outliers. From the plots of the individual sand production, it is apparent that the main production was coming from Layers 2 and 4 from day 1 until day 576. From then on, Layer 3 started to dominate the production contribution and all three layers were contributing almost equal production. The production decline was almost the same for Layers 2 and 4 as evident from their gas productivity indices. Layer 1 had the smallest flow contribution and the lowest decline rate which can be attributed to its low *kh* value.

The OGIP values obtained from the LSFM and the CWM show a very close match. This time, the OGIP of the layers calculated from the LSFM is slightly higher than that of the CWM.